King Saud University

Arabian Journal of Chemistry

www.ksu.edu.sa
www.sciencedirect.com

ORIGINAL ARTICLE

Value-added synthesized acidic polymer nanocomposite with waste chicken eggshell: A novel metal-free and heterogeneous catalyst for Mannich and hantzsch cascade reactions from alcohols

Pouya Ghamari kargar *, **Faeze Bakhshi, Ghodsieh Bagherzade** *

Department of Chemistry, Faculty of Sciences, University of Birjand, Birjand 97175-615, Iran

Abstract The removal of metals from chemical reactions has raised growing concerns for conserving natural resources and environmental safety. Therefore, it is necessary to expand simple procedures that use eco-friendly materials with high elimination capacities. In this paper, we have synthesized a new nanocomposite material in which eggshell membranes act as nucleation sites for $CoFe_2O_4$ nanoparticle precipitation in the attendance of an external magnetic field. In the next step anchoring a chlorosulfonic acid on the surface of eggshell-coated magnetic nanoparticles as solid waste was transformed into a magnetic biomaterial, green, cheap, and environmentally friendly catalyst ($CoFe_2O_4$@Eggshell@SO_3H). Techniques such as FT-IR, VSM, FESEM, TEM, EDX, XRD, and TGA were used to characterize the as-synthesized catalyst. The catalytic property of the as-prepared catalyst was examined in the synthesis of 2,4,6-triarylpyridine, β-aminocarbonyl, and 2-amino-4,6-diphenylnicotinonitrile via alcohol-based oxidation. Excessive yield, quick reaction time, solvent-free condition, waste to wealth, and optimization with the layout of the experiment are the important advantages of the present work. Taken collectively, these results offer the conversion of wastage to fortune products around the world and utilization in organic metamorphosis.

© 2023 The Author(s). Published by Elsevier B.V. on behalf of King Saud University. This is an open access article under the CC BY-NC-ND license (http://creativecommons.org/licenses/by-nc-nd/4.0/).

* Corresponding authors at: Department of Chemistry, Faculty of Sciences, University of Birjand, Birjand 97175-615, Iran.
E-mail addresses: P.ghamari71@gmail.com, P.ghamari71@birjand.ac.ir (P. Ghamari kargar), Bagherzadeh@birjand.ac.ir, gbagherzade@gmail.com (G. Bagherzade).

Peer review under responsibility of King Saud University.

Production and hosting by Elsevier

1. Introduction

Magnetic nanoparticles are an interesting class of nanomaterials that have been widely investigated for use in many technological applications. Nowadays, magnetic nanoparticles are one of the influential factors in the nanomaterial family, which have been extensively employed in different sciences, consisting of drug shipping, (Zhang et al., 2020) sickness recognition, (Kang et al., 2019) water desalination, (Hajizadeh et al., 2020) environment scrubbing, (Taheri-Ledari et al.,

2020) and chemical catalysis (Ghamari kargar et al., 2021a; Ghamari kargar and Bagherzade, 2021a; Khashei Siuki et al., 2020). Furthermore, these magnetic nanoparticles have attracted interest within the discipline of biomedicine, because MNPs have been used to induce heating for hyperthermia treatments, to provide contrast effects for magnetic imaging, and for the remote control of targeted drug delivery (Bagherzade et al., 2021; Bakhshi et al., 2021; Karaagac et al., 2019; Sharifianjazi et al., 2020). Recently, numerous iron oxides have been known that typically refer to three types: α-Fe_2O_3 (hematite), γ-Fe_2O_3 (maghemite), and Fe_3O_4 (magnetite). These compounds form an outstanding category of functional materials that can be applied in various fields. Among all iron oxides, Fe_3O_4 has attracted more attention due to its superior magnetic properties. (Alavinia and Ghorbani-Vaghei, 2022; Zafari et al., 2021) In the last two decades, research on Fe_3O_4 nanoparticles has achieved significant progress not only in the synthesis of homogeneous core magnetic nanoparticles Fe_3O_4 nanoparticles but also in the preparation of advanced nanoarchitectures (composites, core–shell, functionalized surfaces, etc.) and the use of these nanomaterials in different fields. (Ghamari Kargar

et al., 2022c; Ghamari Kargar et al., 2022d; Ghamari Kargar and Bagherzade, 2021c) Fe_3O_4 has attracted more attention than other iron oxides or ferrite spinel oxides (MFe_2O_4 with M = Co, Ni, Mn, Cu, etc.) because of its superior magnetic properties, electronic conductivity, and biocompatibility. (Xie et al., 2021; Xie and Wang, 2021; Khashei Siuki et al., 2022) In this sense, ferrite spinel oxides with superparamagnetic behavior, are presently utilized in drug transport, microwave devices, catalytic activity toward oxidative reactions, magnetic imaging, photocatalytic activity, magnetic data storage, and multi-component reactions (Radmansouri et al., 2018; Ghamari Kargar et al., 2021c). Ferrites are compounds with different and useful physical properties along with high chemical stability and low production cost is known as valuable materials. Ferrites' structure may be exclusive from garnet, hexagonal, and spinel, based on their preliminary crystal lattice (Milam-Guerrero et al., 2019; Kiani et al., 2020). Among diverse structures, spinel ferrites are the most penchant class and are divided into normal and inverse forms among these groups, cobalt ferrite NPs ($CoFe_2O_4$) have been of great fondness owing to their potential for being used in different fields (Scheme 1) (Rouhani
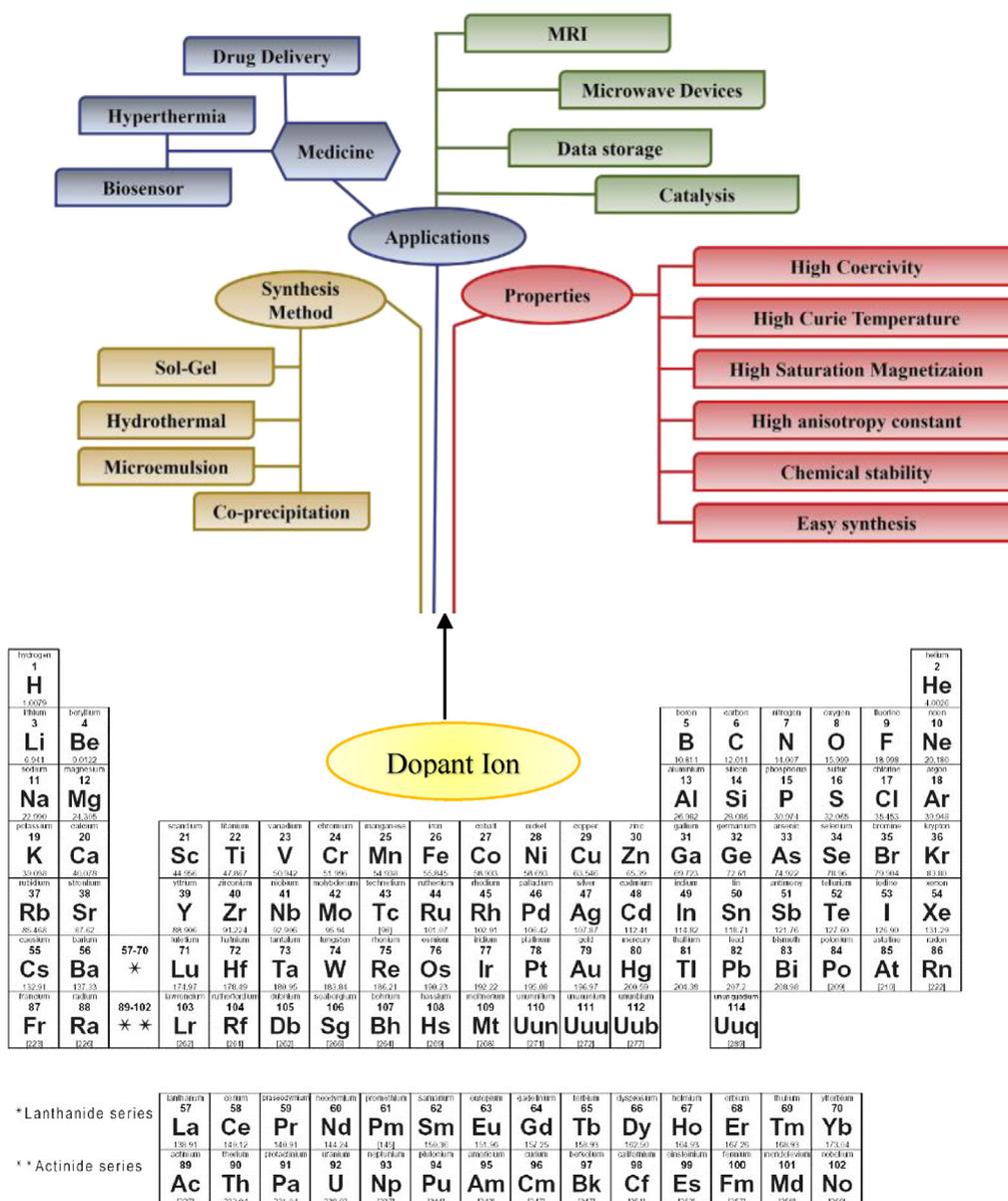

Scheme 1 Synthesis techniques, properties, and applications of $CoFe_2O_4$.

et al., 2018; Jabbar et al., 2020; Londoño-Calderón et al., 2020; Pi et al., 2020; Ghamari Kargar and Bagherzade, 2021b; Ghamari Kargar et al., 2020b). Lately, ferrite magnetic nano-catalysts have attracted the consideration of many researchers because of their high activity, availability, selectivity, low toxicity, excellent reusability, large surface area, and easy separation (Bagherzade and Khashei Siuki; Bita Baghernejad, 2021). Ferrite magnetic nanoparticles can be functionalized with organic and inorganic compounds such as silica, (Afzalimir et al., 2020; Bakherad et al., 2018) surfactants, (Lu et al., 2008) polymers, (Ghamari kargar et al., 2021d; Ghazavi et al., 2022) cellulose, (Ghamari kargar et al., 2020c) carbon, (Safari and Javadian, 2015) chitosan, (Mohammadi et al., 2014) pectin, (Ghamari Kargar and Bagherzade, G., Ghasemi, 2021) due to their high surface-to-volume ratio. The coating layer on magnetic nanoparticles can be barricaded from aggregation or oxidation; and their stability can be enhanced.

Another method of immobilization is using bio-derivative materials as environmentally benign supports. In current years, there has been a splendid upsurge of interest in the application of biowaste materials consisting of eggshell waste. Consistent with the literature, chemicals composition of eggshells are $CaCO_3$ (94 %), organic matter (4 %), $MgCO_3$ (1 %), and $Ca_3(PO_4)_2$ (1 %) (Stadelman and Schmieder, 2002). Low-fee eggshell waste has been used extensively as probable support, catalyst, bone replacement, inexpensive adsorbent for removal of ionic pollutants and dyes from the aqueous medium, coating pigments for inkjet printing paper, the starting material for preparing calcium phosphate bio-ceramics and efficient bio-templates in recent years due to their high catalytic activity, reusability, ease of handling, and benign character (Fakhimi et al., 2022; Fatemeh Kamali, 2021; Ji et al., 2021; Kalantari et al., 2022). The use of waste eggshells as an aid not only provides a powerful and environmentally sound method for the production of heterogeneous catalysts but also enables

the production of economically and ecologically friendly heterogeneous catalysts. Currently, waste eggshell has been used as a catalyst for the preparation of dimethyl carbonate, biodiesel synthesis, and lactose isomerization (Ghani et al., 2023; Rezayati et al., 2022). Meditation some benefits of Fe_3O_4-eggshell catalysts consisting of the fact that they are simple to find, their cheap supports, and the catalyst preparation method, these catalysts have been subjected to study by many researchers. Environmental compatibility, simple accessibility, and Biodegradability are three established features of these catalysts that categorize them as green catalysts (Talha and Sulaiman, 2016). The placement of acidic groups on the ferrite magnetic nanoparticles have been used as catalyst shells in different functional groups metamorphosis because catalysis has played a first-rate role in preventing pollution in our environment. One of the best Brønsted acid catalysts, which is highly active in acid-catalyzed reactions, is sulfuric acid. Even though liquid sulfuric acid is used annually in critical chemical processes, it travails from several damages such as purification of the product, troublesome separation of sulfates, and neutralization of sulfuric acid that produces a large amount of waste which also involves significant energy and material use. Consequently, because of the economic pressures and the stringent environmental standards, tons of attention have been directed toward immobilized sulfuric acid on a solid support to simple purification of the products, effective separation of catalyst, and reduction waste. Toward this aim, many support materials inclusive of polymers, (Caetano et al., 2009) amorphous and mesoporous carbon, (Hayati et al., 2018; Zareyee et al., 2013) mesoporous silica (Morales et al., 2011; Zareyee and Serehneh, 2014) and amorphous silica (Gu et al., 2007) are regularly used for immobilization of sulfuric acid, which can be separated with the aid of conventional separation techniques along with filtration and centrifugation. They screen the benefits of easy catalyst recycling from the liquid reaction media, green
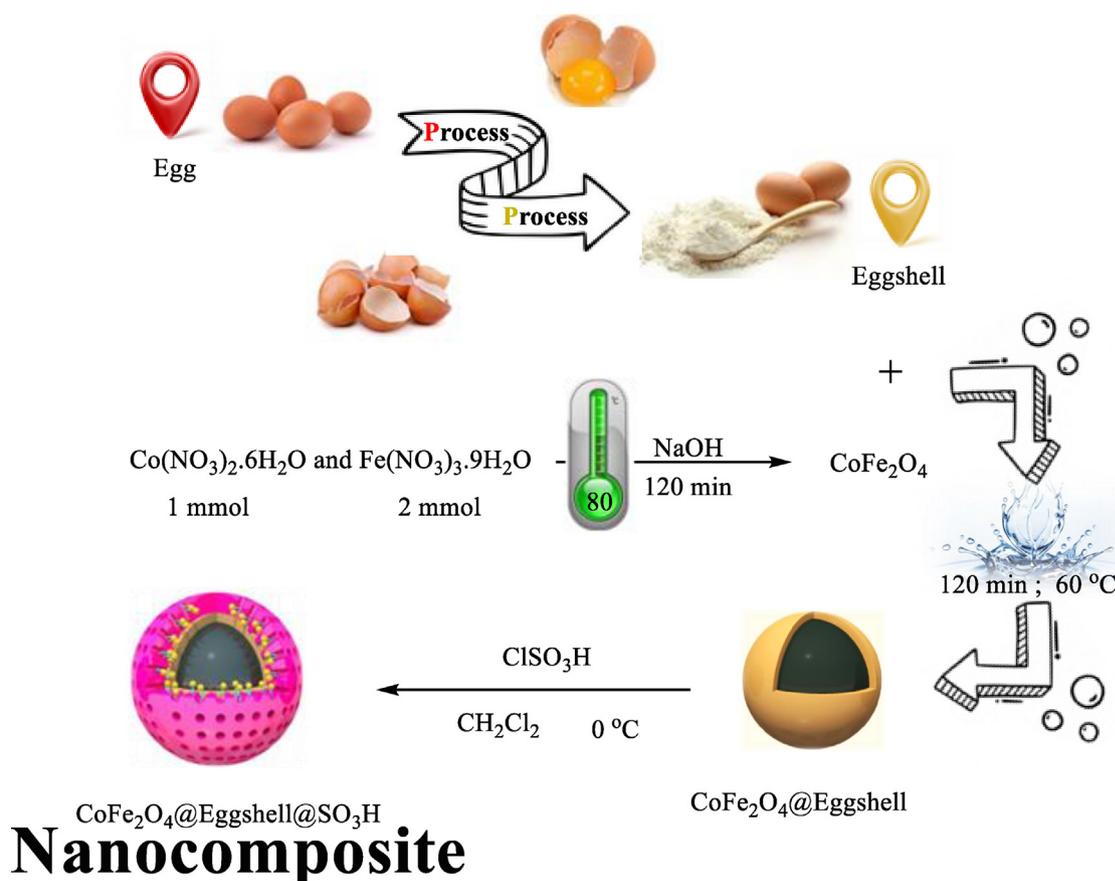
Scheme 2 Schematic representation of synthesized $CoFe_2O_4@Eggshell@SO_3H$ nanocomposite.

chemical method, least corrosion, reusability, and increased product selectivity in multi-component reactions (Rostamnia and Doustkhah, 2015; Sobhaniaragh et al., 2021).

Multicomponent reactions (MCRs) refer to one-pot, convergent chemical reactions using more than two starting materials in which the final product retains a significant fraction of all starting materials. This state-of-the-art approach has emerged as an efficient, cost-effective, and environmentally friendly alternative for the sequential multi-step synthesis of diverse biologically active pharmacophores. (Sharma et al., 2020; Bakavoli et al., 2005) MCRs show a very high bond formation index (BFI) because several non-hydrogen atom bonds are formed in one synthetic transformation. Rapid chemical reactions and simple experiments are unique features of MCR, leading to diversity-oriented synthesis (DOS) and the complexity of desired end products. MCRs are particularly suitable for preparing large libraries of synthetic molecules with the aim of conducting structure–activity relationship (SAR) studies of drug-like compounds as an essential part of research in the fields related to pharmaceutical, agro-chemical, and different industries. (Wang et al., 2019) Under such inspiration in the closing decades, multi-component reactions (MCRs) have been extensively utilized in organic synthesis because of their efficacy for the technology of heterocyclic compounds in a single artificial step. Those reactions constitute very effective chemical generation techniques from each economic and synthetic point of view, and they
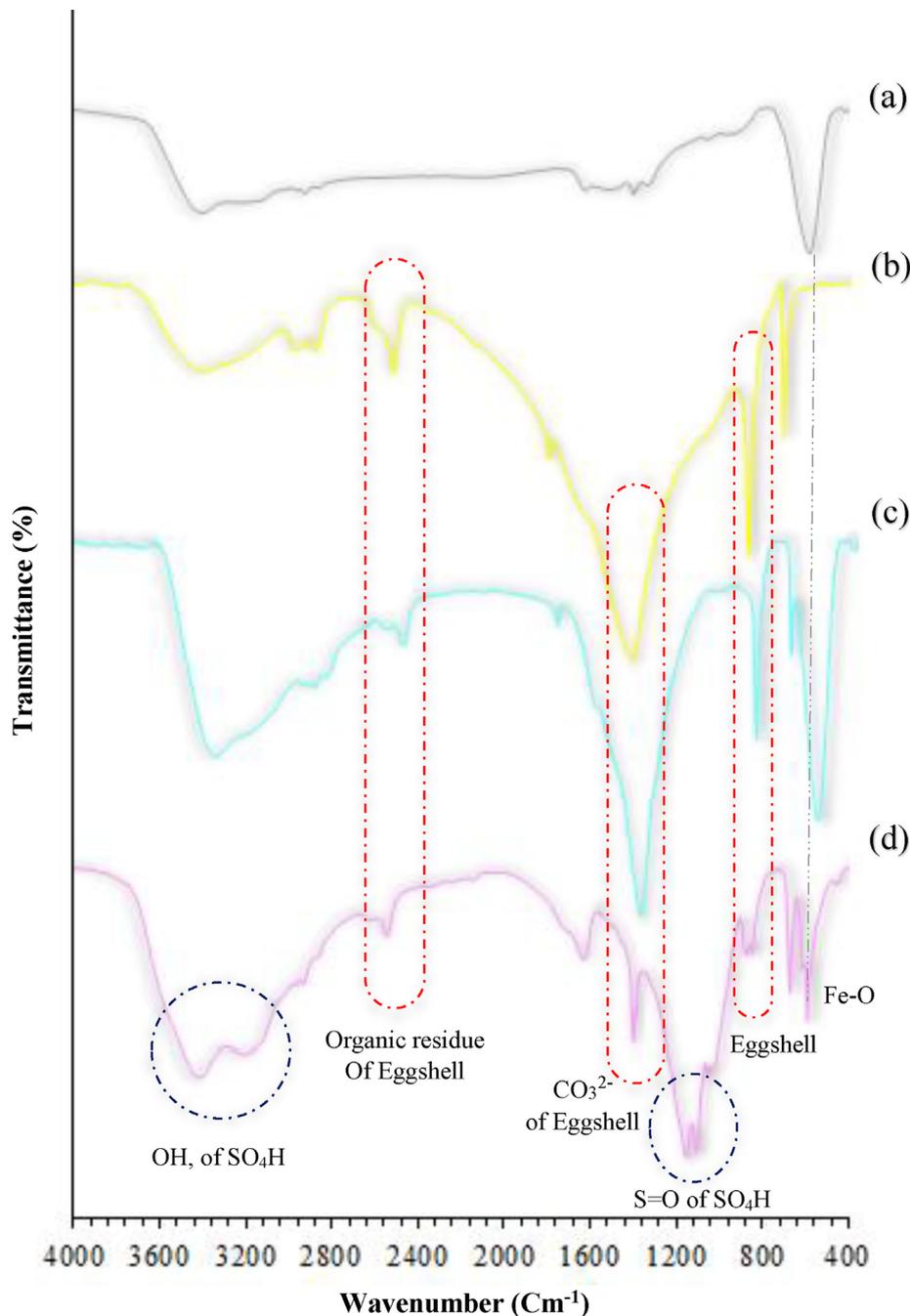

Fig. 1 FT-IR spectra of (a) CoFe$_2$O$_4$, (b) Eggshell, (c) CoFe$_2$O$_4$@Eggshell and (d) CoFe$_2$O$_4$@Eggshell@SO$_3$H nanocomposite.

are one of the maximum influential strategies in green chemistry, business chemistry, and the contemporary drug discovery process (Gholami et al., 2020; Foroughi Kaldareh et al., 2020; Ghamari kargar et al., 2022b). Therefore, discovering of novel MCRs is an interesting topic for synthetic chemistry researchers. Generally, the MCR reactions are carried out in the presence of a homogeneous or heterogeneous catalyst. One of the most important challenges in catalysis nature is the conversion of a successful homogeneous catalyst to a heterogeneous catalyst, as homogeneous catalysts have disadvantages, including disposability, slow reaction speed, and saponification problems due to the presence of fatty acids in the starting materials. On the other hand, solid-supported heterogeneous catalysts have gained significant interest in organic synthesis because of their unparalleled properties, such as high efficiency due to more surface area, easy product/catalyst separation, reusability, low toxicity, higher reaction speed and selectivity, low cost and more stability (Ghamari Kargar et al., 2020a; Naeimi and Nazifi, 2014; Seitllari et al., 2020). Due to these facts, the development of solid-phase catalysts has received increasing attention for synthesis reactions, including MCRs. Currently, the *N*-heterocyclic pyridine compounds have attracted excellent attention in pharmaceutical chemistry due to possessing various activities, which include antiepileptic, vasodilator, antimalarial, anticonvulsant, aesthetic, and agrochemicals like pesticidal, fungicidal, and herbicidal (Ardeshir Khazaei et al., 2020; Nabizadeh and Jamali, 2021; Nagarapu et al., 2007). Pyridine ring systems, specifically 2,4,6-triarylpyridines represent an essential magnificence of heterocyclic compounds due to their specific function in medicinal chemistry (Kim et al., 2004; Reza et al., 2020). Further, the great thermal stabilities of these pyridines have instigated a developing interest in their use as monomeric building blocks in thin films and organometallic polymers (Ghamari kargar et al., 2022a; Hosseini and Khamesee, 2021).

In addition to pyridine, among nitrogen-containing compounds, β-amino carbonyl scaffolding is of increasing importance in organic chemistry of their affluence in a diversity of naturally occurring products and biologically active compounds (Filho et al., 2017). β-amino carbonyl compounds are essential building blocks for the guidance of amino alcohols, peptides, lactams, and precursors to synthesize amino acids and many nitrogen-containing biologically vital compounds (Rezayati et al., 2021; Zhang et al., 2014). Consequently, searching for powerful techniques for synthesizing β-amino carbonyls is an attractive challenge. β-Amino carbonyls have been regarded as considerable targets in organic syntheses. Some of the ways that have been noted for the preparation of β-amino carbonyls are the use of diverse catalysts (Mohammadi Ziarani et al., 2021; Lu and Cai, 2010; Goswami et al., 2013). Each of these techniques can also have its advantages, and blessings; however, it can also be afflicted by apparent drawbacks, which include extended reaction time, complicated work-up, low yield, or risky response conditions. Moreover, many of them are corrosive and risky and frequently reason environmental troubles, which limits their use in the synthesis of nitrogen-containing essential compounds. Subsequently, an environmentally benign technique for the preparation of such compounds is of wonderful problem in synthetic organic chemistry.

Therefore, to keep away from such drawbacks, the development of more simple, green protocols, non-poisonous and 'greener' techniques for synthesizing metal nanoparticles and pyridine and mannish reactions underneath slight situations with averting organic solvents and poisonous reagents remains in call for. Synthesis of pyridine and mannish reactions using environmentally benign materials like alcohols has received increasing attention due to a growing need to develop green technologies. So, in this work, a new and highly effective strategy is used to synthesize novel CoFe$_2$O$_4$@Eggshell@SO$_3$H heterogeneous nanocomposite by using eggshell bio-ceramic and chlorosulfonic acid for coating MNPs via the co-precipitation method. To our knowledge, this is the first report on the green synthesis of CoFe$_2$O$_4$ supported on eggshell waste as a natural and biocompatible nanocomposite. In addition, the catalytic activity of the nanocomposite was investigated in the synthesis of 2,4,6-triphenyl pyridine, β-amino carbonyl, and 2-amino-
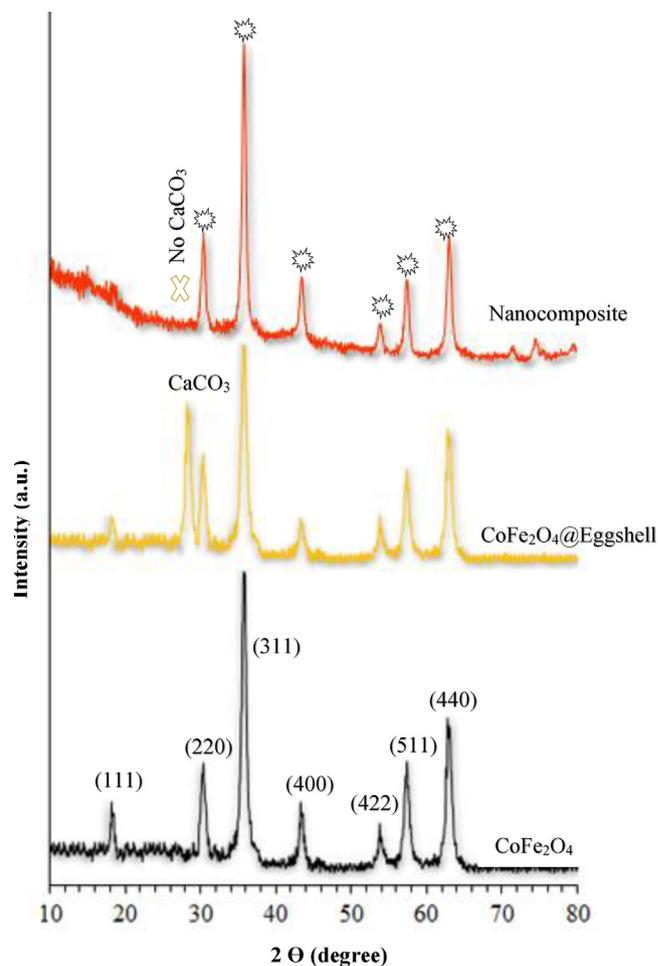

Fig. 2 XRD pattern of (line black) CoFe$_2$O$_4$, (yellow line) CoFe$_2$O$_4$@Eggshell and (orang line) CoFe$_2$O$_4$@Eggshell@SO$_3$H.
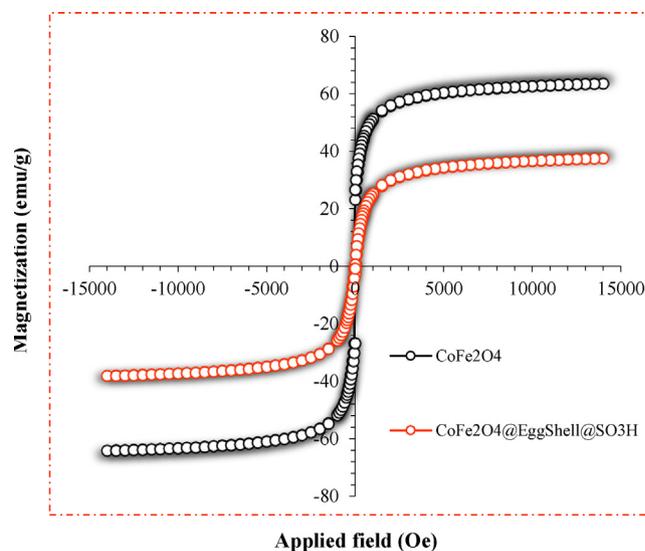
Fig. 3 Magnetization curves of (Θ) CoFe$_2$O$_4$, and (Θ) CoFe$_2$O$_4$@Eggshell@SO$_3$H.

4,6-diphenylnicotinonitrile via one pot multi-component condensation of benzyl alcohol derivatives in solvent and appropriate thermal conditions for the first time. Simple work-up procedures, ease of preparation and facile purification, improved product yields, mild reaction conditions, shorter reaction times, and recyclability of the catalyst are the main advantages of CoFe$_2$O$_4$@Eggshell@SO$_3$H nanocomposite.

2. Experimental

All chemicals and device specifications used are in the supporting information file.

2.1. Preparation of CoFe$_2$O$_4$

The CoFe$_2$O$_4$ ferrite particles were prepared by the chemical co-precipitation method by digestion (Hosseinzadeh et al., 2019). The starting materials were high-purity Co(NO$_3$)$_2$·6H$_2$O and Fe(NO$_3$)$_3$·9H$_2$O, and NaOH was used as the precipitation agent. Firstly, The reaction is described by Co(NO$_3$)$_2$·6H$_2$O and Fe(NO$_3$)$_3$·9H$_2$O with Co:Fe atomic ratio of 1:2 was dissolved in deionized water by gentle heating. Then, the aqueous mixture was slowly poured into a well-stirred NaOH solution and stirred for several minutes. The digestion was performed at 80 °C for 120 min. During digestion, the particles grew and evolved into a spherical structure. After digestion, the gelatinous precipitate was filtered and washed several times using deionized water and EtOH until the pH value of the solution became neutral. Finally, the gelatinous precipitate was dried at 80 °C in the air to form a powder sample.

2.2. Preparation of eggshell powder

The eggshell was prepared according to the procedure described in the literature. (Nasrollahzadeh et al., 2016) 20 g of eggshells were collected at home and washed with warm water, and then the adhering membrane was separated manually. The eggshells were boiled in distilled water for 2 h and then washed with distilled water. After the drying of eggshells in an oven (120 °C for 2 h), the size of the eggshell was reduced using a cutting mill. Eggshells contain organic impurities that should be removed before use, so that 100 mL CH$_2$Cl$_2$ was added to the eggshell and sonicated for 2 h. Finally, the powder was separated using filtration and dried in an oven for 12 h.

2.3. Preparation of CoFe$_2$O$_4$@eggshell

2 g of the eggshell powder was added to the 100 mL water and stirred for 20 min at room temperature, and then 1 g from as-synthesized CoFe$_2$O$_4$ was added to the mixture. The mixture was dispersed for 15 min using ultrasound and stirred for 2 h at 60 °C. There are two kinds of intermolecular interactions between CoFe$_2$O$_4$ and CaCO$_3$, which are electrostatic, electrostatic-electrodynamics, and electrodynamics. The intermolecular interactions are strong enough to prevent the separation of eggshells from the CoFe$_2$O$_4$, so experimental results confirm this. Finally, the CoFe$_2$O$_4$@Eggshell was filtered and dried in an oven.

2.4. Preparation of CoFe$_2$O$_4$@eggshell@SO$_3$H nanocomposite

After the dispersion of CoFe$_2$O$_4$@Eggshell (1.5 g) in 100 mL CH$_2$Cl$_2$ for 15 min, 1.0 mL chlorosulfonic acid (ClSO$_3$H; density: 1.75 g/cm^3) dissolved in CH$_2$Cl$_2$ (20 mL) was added dropwise to the dispersed solution at 0 °C. The mixture was stirred for 24 h at room temperature. The CoFe$_2$O$_4$@Eggshell@SO$_3$-H product was separated by a permanent magnetic field and washed three times with absolute ethanol. The resulting nanocomposite was dried in an oven for 12 h, then characterized by FT-IR analyses.

The reaction between eggshell (CaCO$_3$) and ClSO$_3$H is as (Khazaei et al., 2018):

$$2ClSO_3H \ + \ CaCO_3 \ \rightarrow \ CaCl_2 \ + \ Ca\,(HSO_4)_2 \ + \ CO$$

$$(1)$$
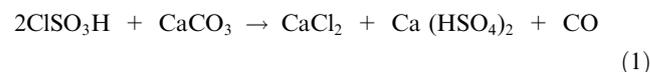
2.5. General procedure for the synthesis of 2,4,6-triarylpyridine derivatives

To a solution of benzyl alcohol (1 mmol), acetophenones (1.2 mmol), ammonium acetate (1 mmol), and 0.05 g (0.4 mol%) of nanocomposite CoFe$_2$O$_4$@Eggshell@SO$_3$H was stirred at 80 °C under solvent-free condition for an appropriate time. After completion of the reaction (monitored by TLC), the reaction mixture was cooled, eluted with hot EtOH (2 mL) and then the catalyst was separated magnetically. The title compounds were obtained in their crystalline forms by recrystallization of ethanol solution. The recyclability of nanocomposite in this reaction was studied for 5 runs. After completing each run, nanocomposite was separated by external magnet, washed with EtOH, and dried overnight. All compounds were identified by melting point and in some cases, by CHN, and ^{1}H NMR. (See in file Supporting information).

2.6. General procedure for the synthesis of β-amino carbonyl derivatives

To a solution of benzyl alcohol (1 mmol), acetophenones (1.2 mmol), aniline (1 mmol) and 0.08 g (0.5 mol%) of nanocomposite CoFe$_2$O$_4$@Eggshell@SO$_3$H were stirred in 3 mL ethanol at 40 °C for an appropriate time. After completion of the reaction (monitored by TLC), water was added, and the precipitate was collected by filtration and washed with water to give the pure product. The title compounds were obtained in their crystalline forms by recrystallization of ethanol solution. The recyclability of nanocomposite in this reaction was studied for 5 runs. After completing each run, nanocomposite was separated by an external magnet, washed with EtOH, and dried overnight. All compounds were identified by melting point and also in some cases, by CHN, and ^{1}H NMR. (See in file Supporting information).

2.7. General procedure for the synthesis of 2-Amino-4,6-nicotinonitrile derivatives

To a solution of benzyl alcohol (1 mmol), malononitrile (1 mmol), acetophenones (1 mmol), ammonium acetate (2 mmol), and 0.06 g (0.45 mol%) of nanocomposite CoFe$_2$O$_4$@Eggshell@SO$_3$H was stirred in solvent-free condition at
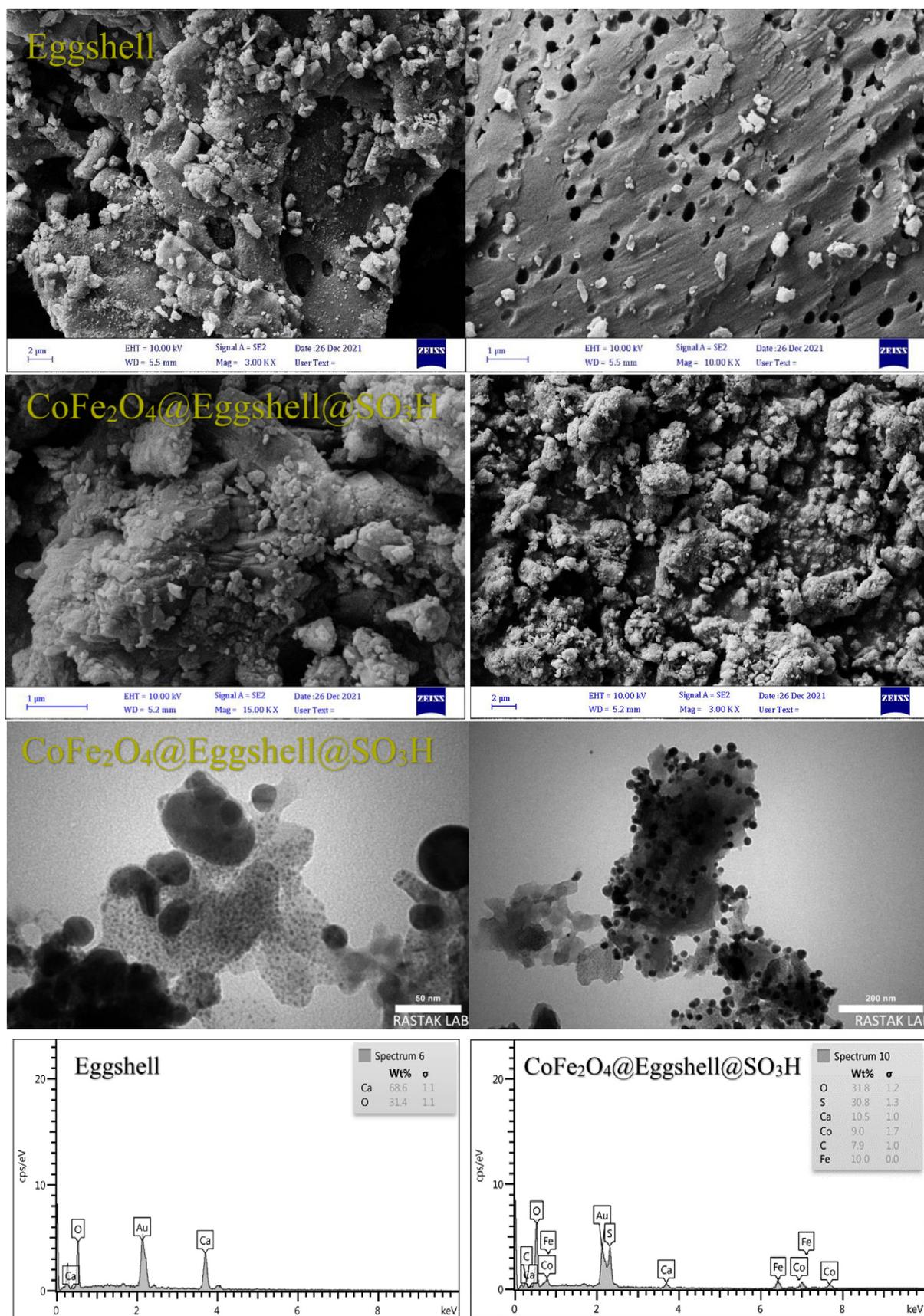
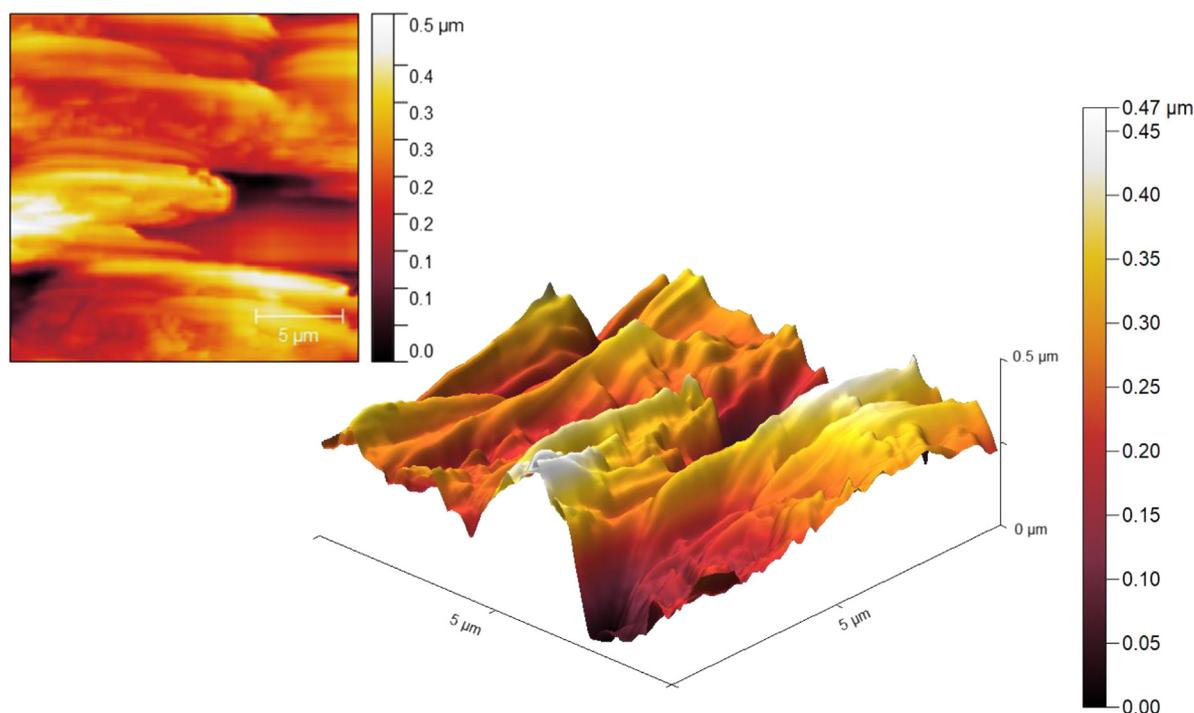**Fig. 4** FESEM, TEM, and EDX images of eggshell, and CoFe$_2$O$_4$@Eggshell@SO$_3$H nanocomposite.

Fig. 5   2D and 3D images of AFM analysis of CoFe$_2$O$_4$@Eggshell@SO$_3$H nanocomposite.
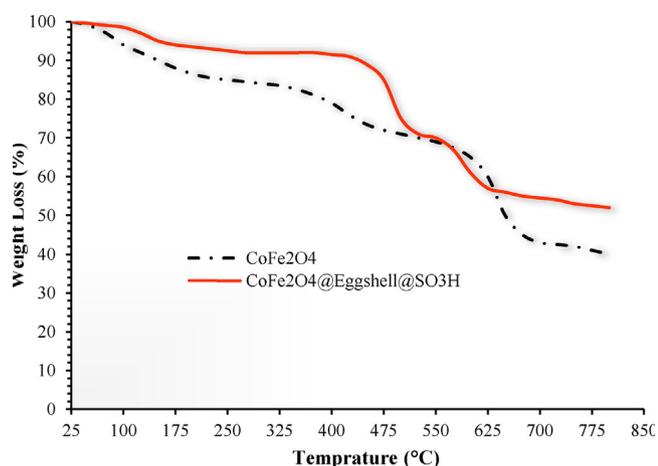
Fig. 6   TGA diagram of (black line) CoFe$_2$O$_4$, and (orange line) CoFe$_2$O$_4$@Eggshell@SO$_3$H.

Table 1   Textural properties of CoFe$_2$O$_4$@Eggshell@SO$_3$H nanocomposite.

| Nanocomposite	Pore volume (cc/g)	Pore radius (Å)	BET Surface area (m^2/g)
CoFe$_2$O$_4$@Eggshell@SO$_3$H	0.06	13.01	17.95

80 °C for an appropriate time. After completion of the reaction (monitored by TLC), water was added, and the precipitate was collected by filtration and washed with water to give the pure product. The title compounds were obtained in their crystalline forms by recrystallization of ethanol solution. The recyclability of nanocomposite in this reaction was studied for 5 runs. After completing each run, nanocomposite was separated by external magnet, washed with EtOH, and dried overnight. All compounds were identified by melting point and also in some cases, by CHN, and ^{1}H NMR. (See in file Supporting information).

3. Result and discussion

Considering our research toward evaluating the catalytic activity of core/shell magnetic nanoparticles natural for the synthesis of organic compounds, (Ghamari Kargar et al., 2020b; Ghamari Kargar et al., 2021b) we structured our study to investigate the suitability of activated CoFe$_2$O$_4$@-Eggshell@SO$_3$H nanocomposite (Scheme 2) as a catalyst for the synthesis of 2,4,6-triarylpyridines and β-amino carbonyl and 2-amino-4,6-diphenylnicotinonitrile. The nano catalyst was characterized by techniques such as FT-IR, XRD, TGA, TEM, FESEM, VSM, DLS, and EDX.

Firstly, the FT-IR spectra of the components of the CoFe$_2$O$_4$@Eggshell@SO$_3$H nanocomposite are shown in Fig. 1. In the CoFe$_2$O$_4$ spectrum, the absorption bands at 588 cm^{-1} are related to the tensile vibrations of the Fe-O bond. The weak and strong peaks observed in the eggshell are present in 713 cm^{-1} and 874 cm^{-1}, which are associated with deformation inside, and outside the plate, respectively, indicating the presence of calcium carbonate (CaCO$_3$). Also, on the other hand, the presence of carbonate, amines and amides, and hydroxyl ions in the eggshell membrane particles was found in Fig. 1, which showed significant peaks at intensities of 1403 cm^{-1}, 1734 cm^{-1}, 2518 cm^{-1}, 2900 cm^{-1}, 3401 cm^{-1}. According to the spectral information of CoFe$_2$O$_4$ and Egg-

Scheme 3 Hantzsh pyridine and Mannich as model reactions.
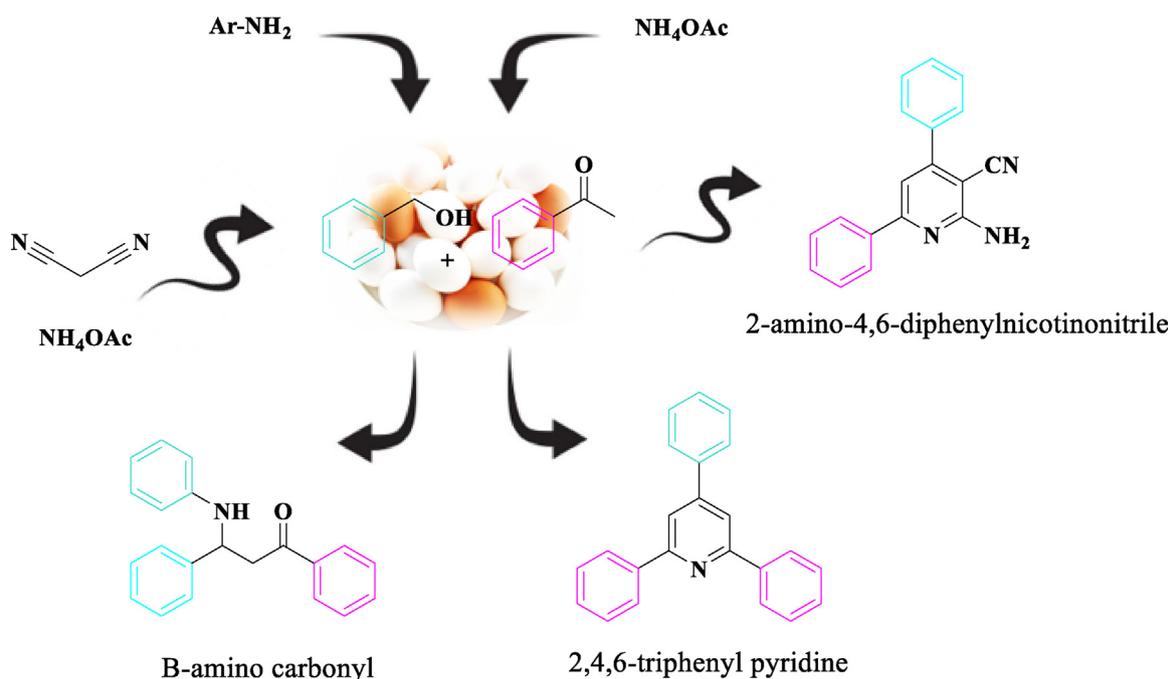
shell, it was observed that in the spectrum $CoFe_2O_4@Eggshell$ (c), all tensile vibrations have appeared. Finally, in the nanocomposite spectrum (d), the tensile vibration of 1152 cm^{-1} corresponds to S=O in the SO_3H group. In addition, it confirms the wavelength of the OH group from 3000 cm^{-1} to 3600 cm^{-1} SO_3H group. These results indicate the conversion of $CaCO_3$ to Ca (HSO$_4$)$_2$ in the synthesis of nanamagnetic catalysts. The functional groups represented by vertical dotted rectangles exist in $CoFe_2O_4$, Eggshell, and $CoFe_2O_4@Eggshell$ (Mahmoudiani Gilan et al., 2021).

The XRD pattern of nanoparticles shown in Fig. 2 has seven distinct peaks for $CoFe_2O_4$ in the regions of (1 1 1) 18/17, (2 2 0) 17/30, (3 1 1) 82/35, (4 0 0) 22/43, (4 2 2) 77/53, (5 1 1) 32/57, (4 4 0) 62/72. This pattern shows that pure $CoFe_2$-O_4 nanoparticles have a spinel structure (Mahhouti et al., 2019). The peak in area 29 indicates calcium carbonate and eggshell layers around $CoFe_2O_4$, which confirms the formation of the $CoFe_2O_4@Eggshell$ core–shell (Mahmoudiani Gilan et al., 2021). It is worth noting that the same seven peaks have appeared for the $CoFe_2O_4@Eggshell@SO_3H$ magnetic nanocomposite. With the disappearance of the calcium carbonate peak and the appearance of a broad peak in the region of 18–25, it shows that the acidic group is stabilized on the eggshell and does not change $CoFe_2O_4$ crystalline phase.

The magnetic properties of $CoFe_2O_4$ and $CoFe_2O_4@$Eggshell$@SO_3H$ were investigated by VSM analysis at room temperature (Fig. 3). According to the obtained diagram, $CoFe_2O_4$ and $CoFe_2O_4@Eggshell@SO_3H$ have superparamagnetic properties. The observed saturation magnetization for $CoFe_2O_4$ and $CoFe_2O_4@Eggshell@SO_3H$ is 63.57 and 37.63 emug^{-1}, respectively. This decrease in magnetism for $CoFe_2O_4@Eggshell@SO_3H$ is due to the stabilization of the eggshell and the acidic group on the surface of the $CoFe_2O_4$.

TEM and FESEM analyzes were used to study the surface morphology and microstructure of $CoFe_2O_4@Eggshell@SO_3$-H nanocomposite. FESEM images were recorded to understand the morphological changes on the surface of the eggshell and magnetic nanocomposite. Fig. 4 show that the eggshell is a coarse porous network. According to the FESEM images, the synthesized $CoFe_2O_4@Eggshell@SO_3H$ are approximately spherical and well dispersed, albeit in some area's larger structures with non-spherical morphology are perceived (Fig. 4). On the other hand, in the TEM image in Fig. 4, the presence and shapes of irregular particles coexisted with spherical particles. The presence of clear bands is known as the edges of the regular crystal lattice, which is attributed to the calcite of the eggshell powder, visible in different directions. In contrast, intertwined spherical particles show the presence of $CoFe_2O_4$.

The results further confirm that the eggshell has high mechanical strength, which makes it a suitable carrier in $CoFe_2O_4$ immobilization. Analysis of TEM and FESEM images shows that the average diameter of nanoparticles is about 30–47 nm. The particle size of the nanocomposite is due to the presence of the eggshell and the stabilized acidic group around the $CoFe_2O_4$ particles as the core. Also, the results of EDX analysis of $CoFe_2O_4@Eggshell@SO_3H$ nanocomposite are shown in Fig. 4 and confirm the presence of carbon, calcium, iron, cobalt, oxygen, and sulfur.

Also, AFM analysis was performed to evaluate the surface properties of $CoFe_2O_4@Eggshell@SO_3H$ nanocomposite. Fig. 5 shows 2D and 3D images of the nanocomposite. According to the 2D image, most of the particles are the same color, which indicates that the particles are about the same thickness. However, the surface porosity, texture and roughness of $CoFe_2O_4@Eggshell@SO_3H$ nanocomposite are shown in the 3D image. In the 3D image, there are various peaks indicate the porous and uneven surface of the magnetic nanoparticles of the eggshell. Therefore, it can be concluded that by modifying the eggshell with magnetic nanoparticles and
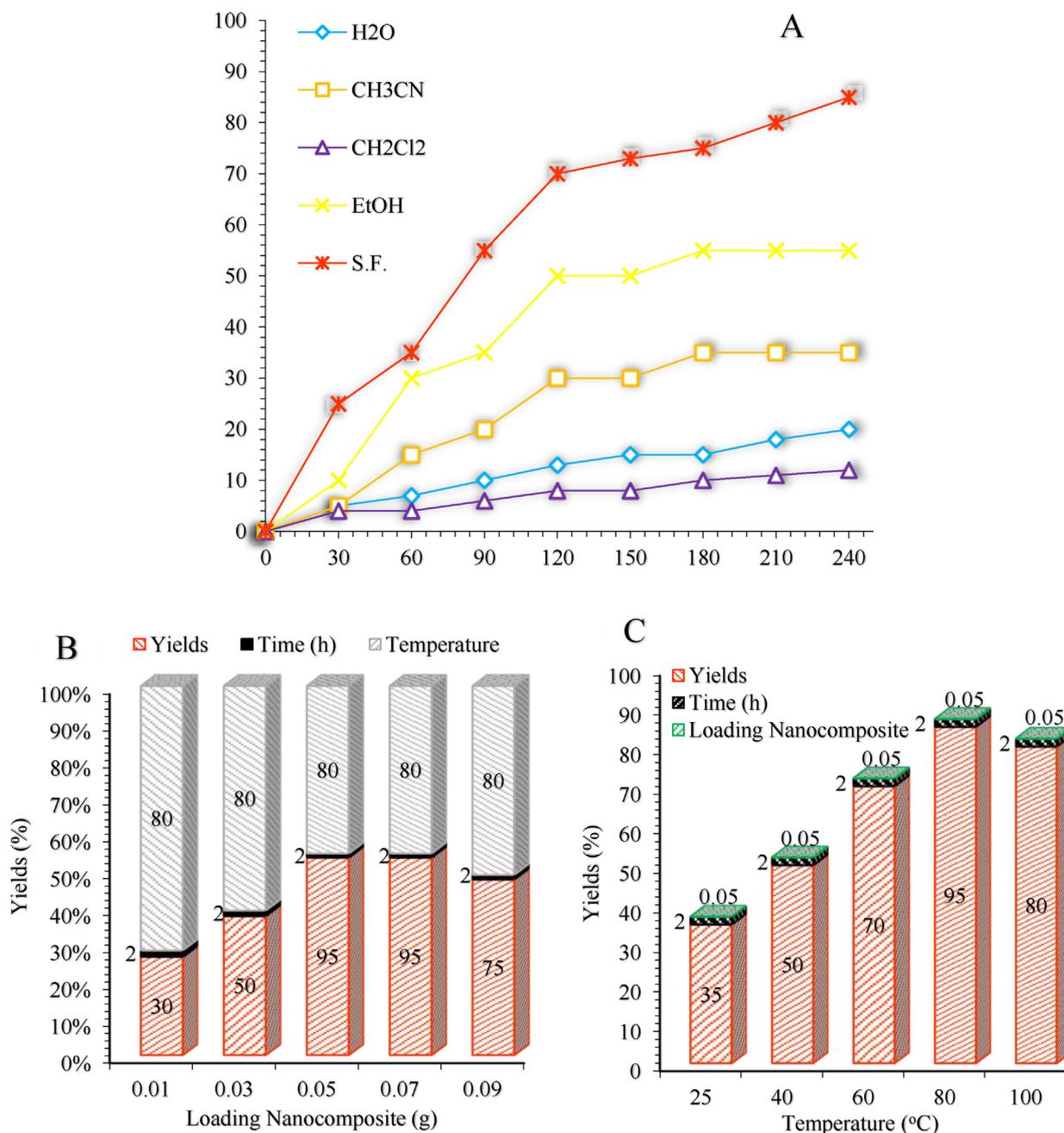
Fig. 7 The screening effect of the solvent, temperature, and catalyst on the 2,4,6-triarylpyridine reaction. Reaction conditions: Benzyl alcohol (1 mmol), Acetophenone (2 mmol), Ammonium acetate (1 mmol), Solvent, Temperature, Catalyst, and Air as the oxidant.

SO_3H group, the number of pores and surface roughness increases.

The thermogravimetric analysis (TGA) of $CoFe_2O_4@$-Eggshell@SO_3H was used to determine the thermal stability and content of organic functional groups on the surface of magnetic nano particles (Fig. 6). Fig. 6 shows the TGA curve for the $CoFe_2O_4@$Eggshell@SO_3H nanocomposite in the temperature range of 25–800 °C. A weight loss of 5 % at temperature below about 200 °C is related to the desorption of water molecules from the nanocomposite surface. In addition, the nanocomposite is stable up to 450 °C, and the weight loss from 450 to 650 °C is related to the decomposition of organic mat-

ter. The eggshell stabilized on the surface of $CoFe_2O_4$. Fig. 4 shows that the eggshell is stable up to 450 °C and is suitable for reactions that are stable at this temperature.

The specific surface area and pore size distributions of the nanocomposite were obtained from BET multi-point and single-point methods using N_2 adsorption–desorption isotherm data (according to the Barrett–Joyner–Halenda method). All the parameters are summarized in Table 1.

After catalyst characterization, we structured our study to check the adaptability of $CoFe_2O_4@$Eggshell@SO_3H nanocomposite as a heterogeneous catalyst for the synthesis of 2,4,6-triarylpyridines and β-amino carbonyl, and 2-amino-
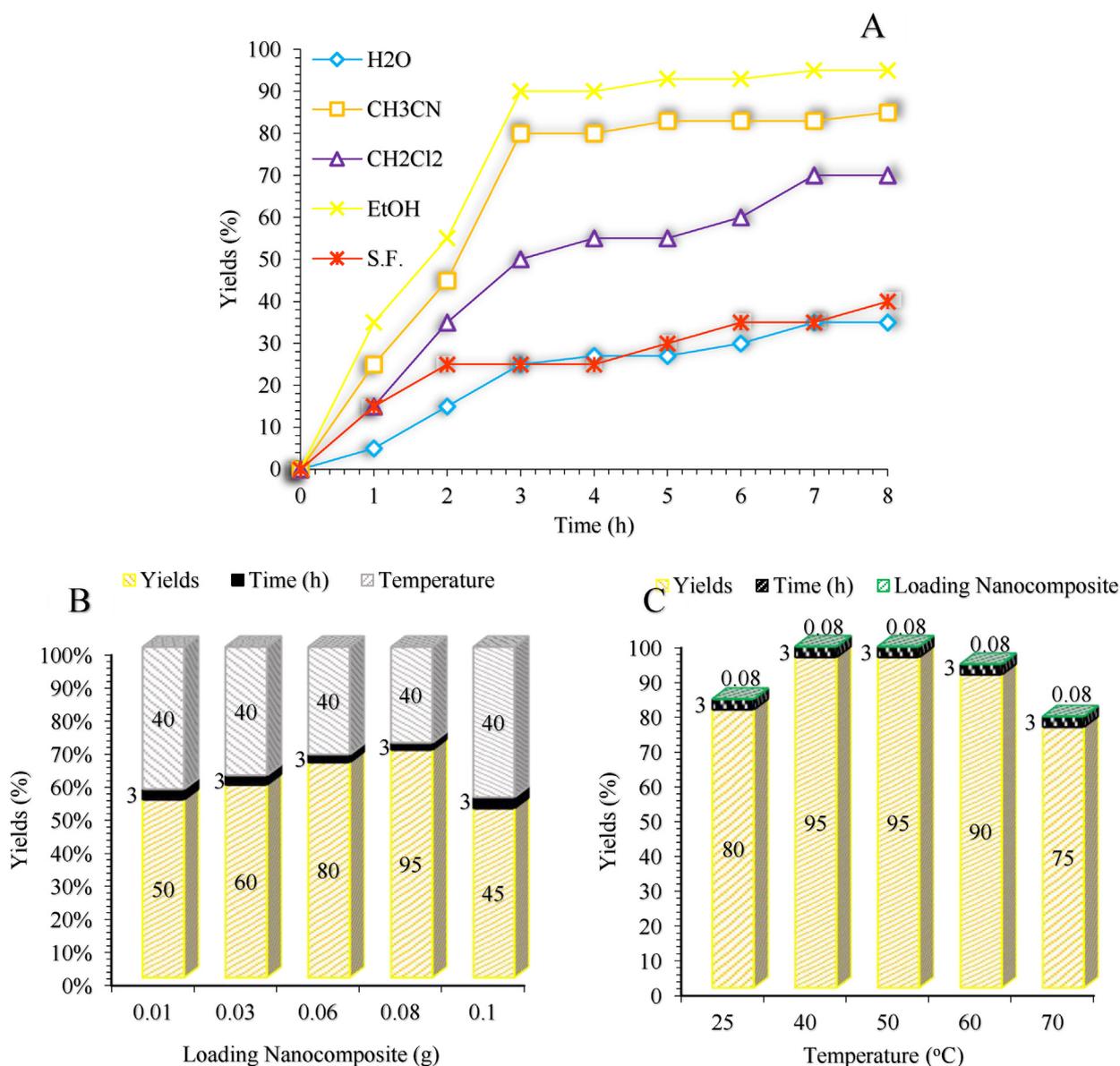
Fig. 8 The screening effect of the Solvent, temperature and catalyst on the β-amino carbonyl reaction. Reaction conditions: Benzyl alcohol (1 mmol), Acetophenone (1.2 mmol), Aniline (1 mmol), Solvent, Temperature, Catalyst, and Air as the oxidant.

4,6-diphenylnicotinonitrile (Scheme 3). The oxidative synthesis of 2,4,6-triarylpyridines, and β-amino carbonyl, and 2-amino-4,6-diphenylnicotinonitrile derivatives using alcohols need both oxidation and acid catalysts. The dual properties of $CoFe_2O_4@Eggshell@SO_3H$ nanocomposite, oxidation capability and acidic property made these catalysts capable of being used in both oxidation, and synthetic sections of the reactions. Finally, the effect of the solvent on time, catalyst loading, and temperature for all three of the model reaction was assessed (Figs. 7-9).

We choose the reaction of benzyl alcohol, and acetophenone, and ammonium acetate as the model 2,4,6-triarylpyridines reaction (Scheme 4). The study of the influence of the solvent, as well as its absence, illustrated that solvent free conditions as green and sustainable reaction conditions rendered the best results (Fig. 7a). To optimize the reaction catalyst, an amount of 0.05 g was found to minimize the

2,4,6-triarylpyridine formation (Fig. 7b). Screening the amount of the catalyst illustrated that decreasing the catalyst amount from 0.07 g to 0.05 g led not to a decrease in the yield of the product. But weaker activity was obtained by further reducing the amount of catalyst (Fig. 7b). Also, a further increase in the amount of catalyst did not have any significant effects on the product yield. Finally, the temperature dependency of the model reaction was investigated (Fig. 7c) and found that the reaction proceeded efficiently under 80 °C.

With an optimized catalytic system in hand (Fig. 7), to develop the scope of the reaction, a wide range of alcohols, acetophenone and ammonium acetate was subjected to nanocomposite reaction under the optimized conditions (Table 2). In all cases, aromatic alcohols with substituents carrying either electron-withdrawing or electron-donating groups reacted effectively and gave the goods correctly yields (Table 2). It was found that aromatic aldehydes with electron-

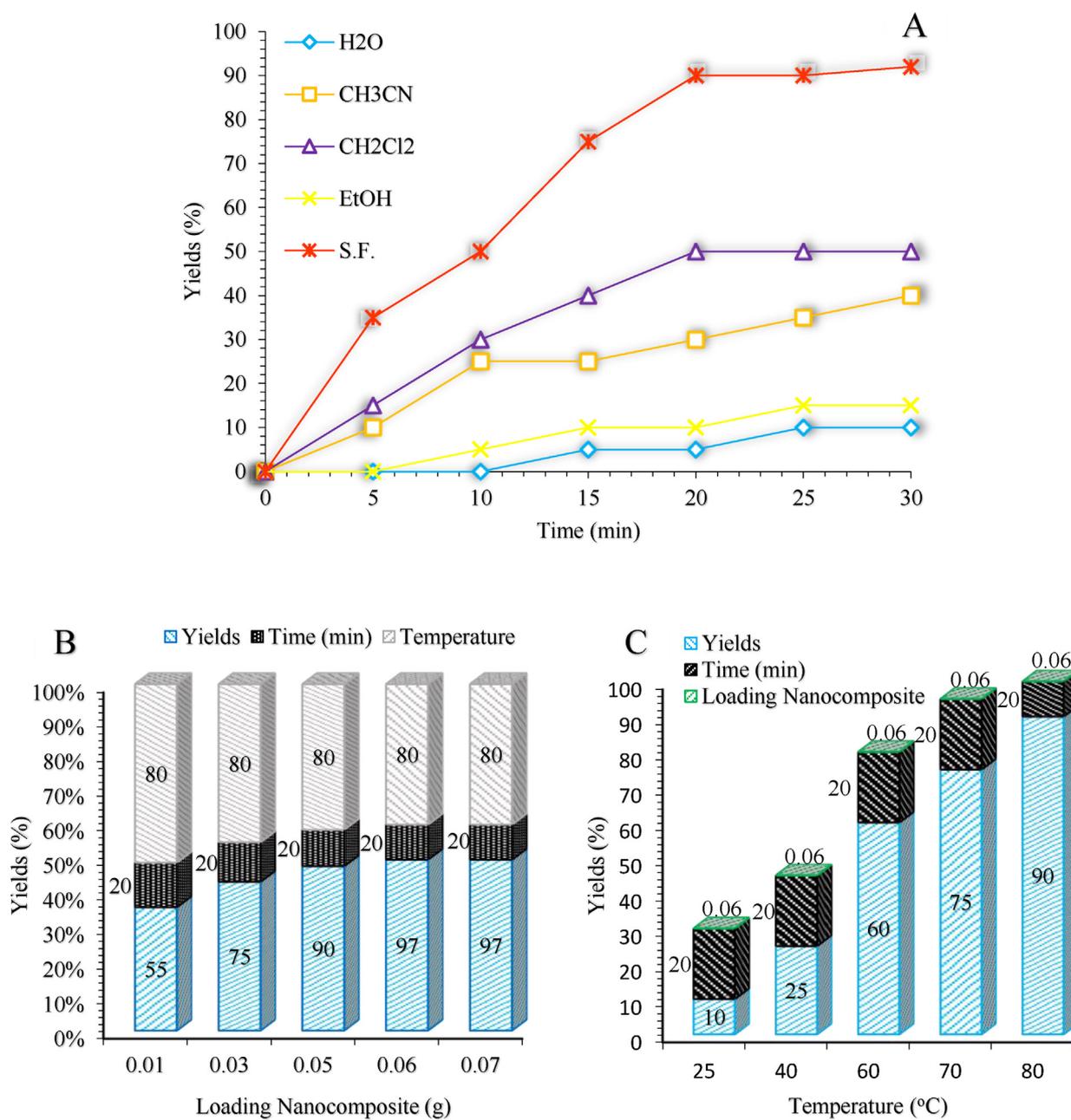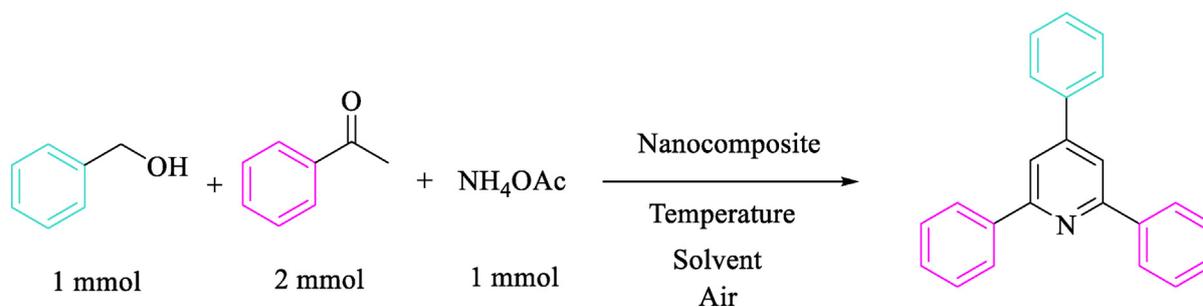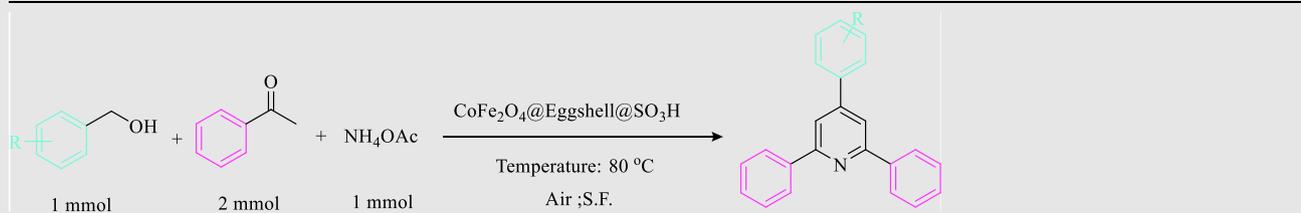**Fig. 9** The screening effect of the Solvent, temperature and catalyst on the 2-amino-4,6-diphenylnicotinonitrile reaction.

Scheme 4 Schematic illustration of the 2,4,6-triarylpyridines as the model reaction by $CoFe_2O_4$@Eggshell@SO_3H.

Table 2 Synthesized different 2,4,6-triarylpyridine derivatives. [a.]

Entry	Alcohols	Time (h)	Yield (%)	m.p. ($^{\circ}$C)	
				Obtained	Reported [ref.]
1	H	120	95	135–137	135–138 (Tabrizian et al., 2015)
2	*para*-F	120	95	178–180	New
3	*para*-Cl	90	95	122–124	123–124 (Tabrizian et al., 2015)
4	*para*-Br	75	97	166–168	165–166 (Tabrizian et al., 2015)
5	*para*-OH	90	92	197–198	196–198 (Tabrizian et al., 2015)
6	*para*-MeO	150	96	100–102	100–101 (Tabrizian et al., 2015)
7	*para*-Me	130	93	125–128	127–129 (Tabrizian et al., 2015)
8	*para*-NO$_2$	100	97	194–196	194–195 (Tabrizian et al., 2015)
9	orto-NO$_2$	120	95	190–192	New
10	orto-Cl	100	95	115–118	115–117 (Tabrizian et al., 2015)

[a] Reaction conditions: Benzyl alcohol (1 mmol), Acetophenone (2 mmol), Ammonium acetate (1 mmol), S.F., 80 °C, Catalyst (0.05 g), Air as the oxidant.

withdrawing groups reacted faster than those with electron-donating groups, as expected. These results justified one more time the efficiency of the nanocomposite.

In subsequent examination, optimization of reaction conditions was carried out in the β-amino carbonyl three-component reaction of benzyl alcohol, acetophenone, and aniline in various solvents, and the presence of temperatures and different amounts of catalyst (Scheme 5). Based on the literature survey, as indicated in Fig. 8a, the efficiency and the yield of the model reaction in EtOH were higher than those

obtained in other solvents. To extend the optimization of the prepared catalyst, the best results related to the amount of nanocomposite, and the temperature are shown in Fig. 8b and Fig. 8c.

To research the generality of this protocol and based on the above-optimized endings, we explored the scope and limitations of this favorable reaction by varying the structure of the benzyl alcohol component. In this attempt, diverse benzyl alcohol derivatives were successfully produced using acetophenone, and aniline in the presence of a catalytic amount of
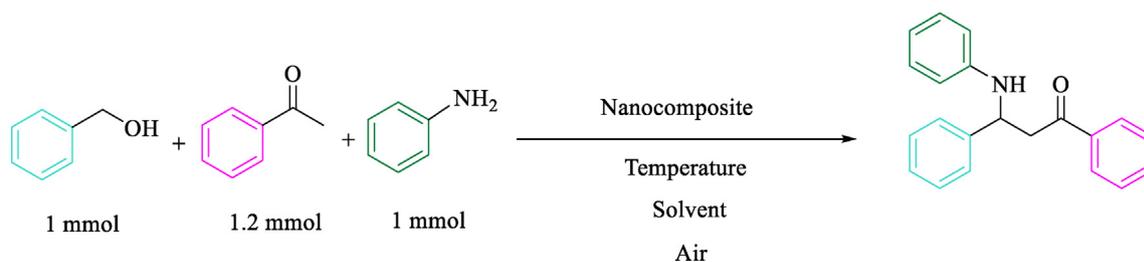
Scheme 5 Schematic Illustration of the β-amino carbonyl as the model reaction by CoFe$_2$O$_4$@Eggshell@SO$_3$H.
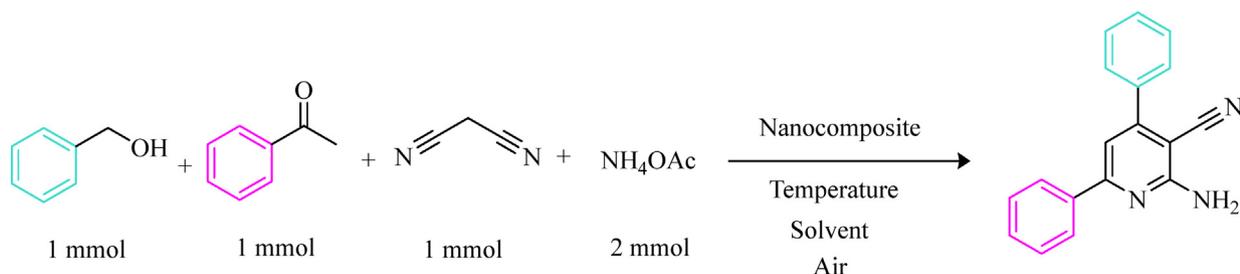
Scheme 6 Schematic illustration of the 2-amino-4,6-diphenylnicotinonitriles as the model reaction by CoFe$_2$O$_4$@Eggshell@SO$_3$H.

Table 3 Synthesized different β-amino carbonyl derivatives. [a.]

Reaction scheme: R-substituted benzyl alcohol (1 mmol) + acetophenone (1.2 mmol) + aniline-NH₂ (1 mmol) → with CoFe₂O₄@Eggshell@SO₃H, Temperature: 40 °C, Air ; EtOH → β-amino carbonyl product.

Entry	Alcohols	Time (h)	Yield (%)	m.p. (°C) Obtained	Reported [ref.]
1	H	180	95	168–170	168–169 (Rahmatpour et al., 2019)
2	*para*-F	180	90	103–105	102–104 (Rahmatpour et al., 2019)
3	*para*-Cl	150	95	116–118	117–118 (Kundu and Nayak, 2012)
4	*para*-Br	120	97	128–130	128–129 (Kundu and Nayak, 2012)
5	*para*-OH	150	96	182–184	181–182 (V.N.K. et al., 2008)
6	*para*-MeO	210	93	150–152	149–150 (Rahmatpour et al., 2019)
7	*para*-Me	180	95	131–133	130–132 (Rahmatpour et al., 2019)
8	*para*-NO₂	150	97	108–110	108–110 (Rahmatpour et al., 2019)
9	orto-NO₂	210	92	123–125	New
10	orto-Cl	180	95	119–121	New

[a] Reaction conditions: Benzyl alcohol (1 mmol), Acetophenone (1.2 mmol), Aniline (1 mmol), EtOH, 40 °C, Catalyst (0.08 g), and Air as the oxidant.

$CoFe_2O_4$@Eggshell@SO_3H in EtOH at 40 °C in excellent yields (Table 3). The process was found to be excellent in terms of yields and times using benzyl alcohol substituted with electron-donating as well as electron-withdrawing moieties.

After the successful synthesis of 2,4,6-triarylpyridine and β-amino carbonyl three-component reactions, we have used our efforts to synthesize the 2-amino-4,6-diphenylnicotinonitrile reaction (Scheme 6). Based on the literature survey, as indicated in Fig. 9, the efficiency and the yield of the model reaction in solvent free condition was higher than those obtained in other solvents (Fig. 9a). To extend the optimization of the prepared catalyst, the best results related to the amount of nanocomposite, and the temperature are shown in Fig. 9b and 9c.

Reaction conditions: Benzyl alcohol (1 mmol), Malononitrile (1 mmol), Ammonium acetate (2 mmol), Acetophenone (1.2 mmol), Solvent, Temperature, Catalyst, and Air as the oxidant.

To research the generality of this protocol and based on the above-optimized endings similar to previous reactions, we explored the scope and limitations of this favorable reaction by varying the structure of the benzyl alcohol component. In this attempt, diverse benzyl alcohol derivatives were successfully produced using acetophenon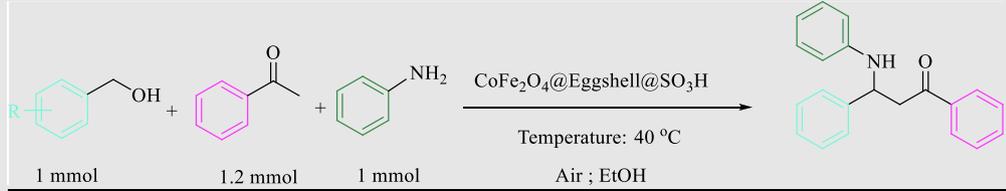e, and aniline in the presence of a catalytic amount of $CoFe_2O_4$@Eggshell@SO_3H in solvent-free condition at 80 °C in excellent yields (Table 4). The process was found to be excellent in terms of yields and times using benzyl alcohol substituted with electron-donating as well as electron-withdrawing moieties.

To illustrate the need for $CoFe_2O_4$@Eggshell@SO_3H nanocomposite for these reactions, an experiment was conducted in the absence of $CoFe_2O_4$@Eggshell@SO_3H nanocomposite, and nanocomposite components $CoFe_2O_4$ alone and $CoFe_2O_4$@Eggshell as analogs of the nanocomposite (Table 5). A simple comparison shows that a desirable activation of $CoFe_2O_4$ occurred by eggshell and SO_3H in the

nanocomposite, and the best yield was obtained in the presence of $CoFe_2O_4$@Eggshell@SO_3H nanocomposite (Table 5; entry 4, 8, 12). In Scheme 7, the catalytic mechanism for $CoFe_2O_4$@-Eggshell@SO_3H-catalyzed formylation is demonstrated on the basis of the findings of previous research. (Taheri et al., 2017; Hosseinzadeh-Khanmiri et al., 2018) At first, the alcohol oxidation is carried out with $CoFe_2O_4$@Eggshell@SO_3H nanocomposite acts as an efficient Brønsted acid catalyst lively active sites especially. $CoFe_2O_4$@Eggshell@SO_3H protonates the carbonyl group and causes it to be more reactive under the nucleophilic attack of oxygen groups. With the release of protons, a mixture reaction is formed to regenerate the catalyst structure through a proton transfer. The synthesized aldehyde enters the synthesis cycle of multicomponent reactions as a starting material. For this purpose, the reactions mechanism of 4,6-triarylpyridine, and β-amino carbonyl, and 2-amino-4, 6-diphenylnicotinonitrile in the presence of $CoFe_2O_4$@ Eggshell@SO_3H was investigated (Scheme 7).

The 2,4,6-triphenylpyridine reaction involves four steps aldol condensation, Michael addition, cyclization, and finally air oxidation. Condensation of an aldehyde and acetophenone forms and aldol product (I); on the other hand, a molecule of acetophenone with ammonia forms an enamine adduct. The addition of enamine to the aldol product, followed by cyclization, gives dihydropyridine (II). Finally, air oxidation afforded the final product (Scheme 7). Also, a plausible mechanism for synthesizing β-amino carbonyl using the $CoFe_2O_4$@-Eggshell@SO_3H nanocomposite is presented in Scheme 7. Initially, we assumed that the reaction occurs via a condensation, between aldehyde and aniline to form intermediate I on the active sites of the $CoFe_2O_4$@Eggshell@SO_3H nanocomposite after dehydration. Next, the imine intermediate activated by as $CoFe_2O_4$@Eggshell@SO_3H nanocomposite Brønsted acid undergoes a nucleophilic attack by enol which in turn converts to the final product and simultaneously releases the catalyst for the next catalytic cycle. This mechanism has been supported by

Table 4 Synthesized different 2-amino-4,6-diphenylnicotinonitrile derivatives. [a.]

| | | | | 1 mmol | 1 mmol | 1 mmol | 2 mmol | $CoFe_2O_4$@Eggshell@SO_3H Temperature: 80 °C Air ; S.F. | |
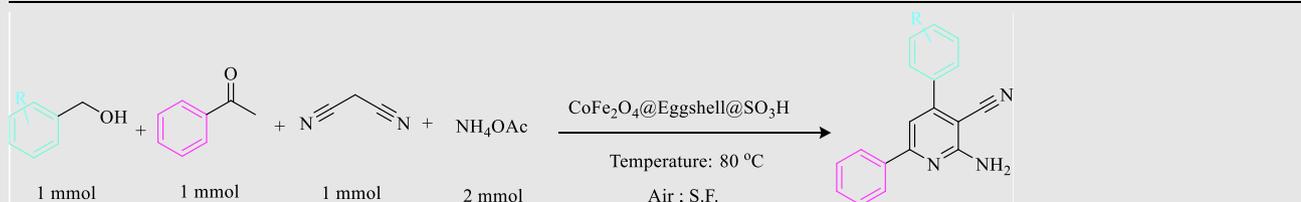
Entry	Alcohols	Time (min)	Yield (%)	m.p. (°C)	
				Obtained	Reported [ref.]
1	**H**	**20**	**97**	**185–187**	186–187 (Heravi et al., 2015)
2	*para*-**F**	**20**	**95**	**211–214**	210–213 (Zolfigol et al., 2016)
3	*para*-**Cl**	**20**	**97**	**170–172**	169–171 (Zolfigol et al., 2016)
4	*para*-**Br**	**15**	**98**	**213–216**	215–218 (Safari et al., 2012)
5	*para*-**OH**	**20**	**95**	**223–225**	225–227 (Erşatır and Yıldırım, 2021)
6	*para*-**MeO**	**25**	**90**	**179–181**	181–182 (Heravi et al., 2015)
7	*para*-**Me**	**20**	**92**	**220–223**	224–227 (Zolfigol et al., 2016)
8	*para*-**NO$_2$**	**15**	**95**	**210–212**	212–213 (Heravi et al., 2015)
9	*orto*-**NO$_2$**	**15**	**95**	**139–141**	140–142 (Rekunge et al., 2021)
10	*orto*-**Cl**	**15**	**96**	**190–192**	193–196 (Khaksar and Yaghoobi, 2012)

[a] Reaction conditions: Benzyl alcohol (1 mmol), Malononitrile (1 mmol), Ammonium acetate (2 mmol), Acetophenone (1.2 mmol), S.F., 80 °C, Catalyst (0.06 g), Air as the oxidant.

Table 5 Comparison of $CoFe_2O_4$@Eggshell@SO_3H nanocomposite performance with analogues of the nanocomposite for 2,4,6-triarylpyridine, β-amino carbonyl, and 2-amino-4,6-diphenylnicotinonitrile reactions.

Reactions	Entry	Catalyst	Time (h)	Yields (%)
2,4,6-triarylpyridine [a]	**1**	–	24	**Trace**
	2	$CoFe_2O_4$ (0.05 g)	4	**35**
	3	$CoFe_2O_4$@Eggshell (0.05 g)	2	**75**
	4	$CoFe_2O_4$@Eggshell@SO_3H (0.05 g)	2	**95**
β-amino carbonyl [b]	**5**	–	24	**Trace**
	6	$CoFe_2O_4$ (0.08 g)	6	**40**
	7	$CoFe_2O_4$@Eggshell (0.08 g)	3	**80**
	8	$CoFe_2O_4$@Eggshell@SO_3H (0.08 g)	3	**95**
2-amino-4,6-diphenylnicotinonitrile [c]	**9**	–	24	**Trace**
	10	$CoFe_2O_4$ (0.06 g)	1	**45**
	11	$CoFe_2O_4$@Eggshell (0.06 g)	0.3	**85**
	12	$CoFe_2O_4$@Eggshell@SO_3H (0.06 g)	0.3	**97**

[a] Reaction conditions: Benzyl alcohol (1 mmol), Acetophenone (2 mmol), Ammonium acetate (1 mmol), S.F., 80 °C, Catalyst (0.05 g), Air as the oxidant.
[b] Reaction conditions: Benzyl alcohol (1 mmol), Acetophenone (1.2 mmol), Aniline (1 mmol), EtOH., 40 °C, Catalyst (0.08 g), Air as the oxidant.
[c] Reaction conditions: Benzyl alcohol (1 mmol), Acetophenone (2 mmol), Ammonium acetate (2 mmol), malononitrile (1 mmol) S.F., 80 °C, Catalyst (0.05 g), Air as the oxidant.

the literature. Finally, a proposed mechanism for the synthesis of 2-amino-4,6-diphenylnicotinonitrile based on scheme 7 is presented. In the first step, the carbonyl aldehyde synthesized with alcohol under aerobic conditions is activated by the nanocomposite $CoFe_2O_4$@Eggshell@SO_3H and reacts. Immediately, malononitrile with activated arylaldehyde via Knoevenagel condensation followed by dehydration to generate intermediate I. On the other hand, ammonia produced from ammonium acetate reacts with activated acetophenone and forms an enamine mediator. Then enamine reacts with

mediator I and forms mediator II. Here, the presence of $CoFe_2O_4$@Eggshell@SO_3H nanocomposite as a catalyst helps to prepare the desired 2-amino-4,6-diphenylnicotinonitrile products after intramolecular cycle, automerization, and aromatization.

For a better assessment of the catalytic performance of $CoFe_2O_4$@Eggshell@SO_3H, a fixed of person catalytic experiments were performed with the employing homogeneous, and heterogeneous Brønsted acid catalysts beneath the equal reaction condition with aromatic aldehydes (Fig. 10). It should be
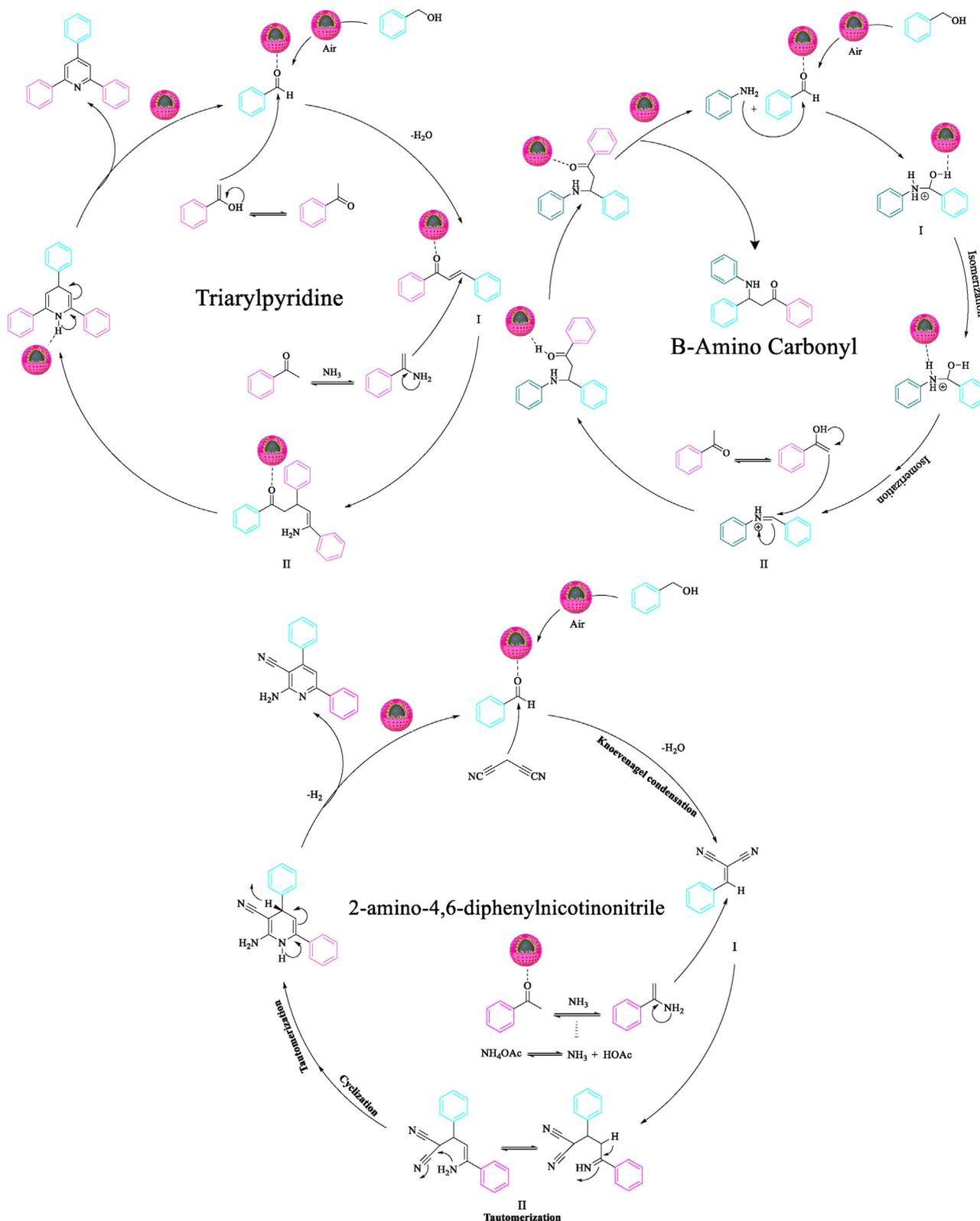
Scheme 7 A plausible mechanism for the preparation of 2,4,6-triarylpyridine, and β-amino carbonyl, and 2-amino-4,6-diphenylnicoti-nonitrile using the CoFe$_2$O$_4$@Eggshell@SO$_3$H nanocomposite.

noted that CoFe$_2$O$_4$@Eggshell@SO$_3$H nanocomposite, for the first time with very suitable conditions and more activity, has prepared Pyridine and Mannich reactions from alcohols (Fig. 10A-B).

CoFe$_2$O$_4$@Eggshell@SO$_3$H nanocomposite can recycle greater without problems from the reaction mixture with an external magnet and reuse numerous times without a decrease in catalytic activity. The recyclability of CoFe$_2$O$_4$
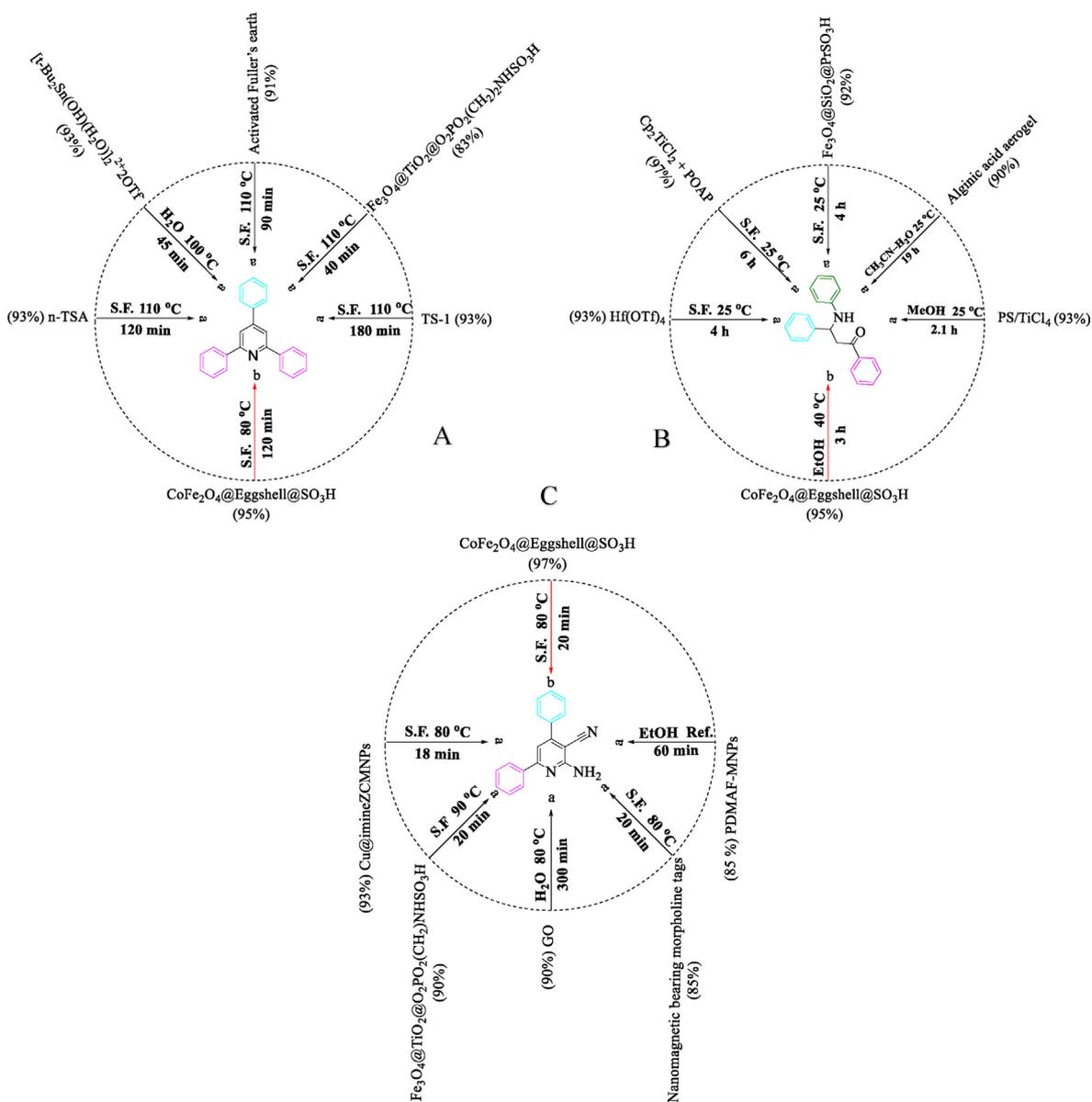
A

[t-Bu₂Sn(OH(H₂O))₂.2⁺2OTf⁻ (95%)] — H₂O 100 °C 45 min a

Activated Fuller's earth (91%) — S.F. 110 °C 90 min a

Fe₃O₄@TiO₂@O₂PO₂(CH₂)₂NHSO₃H (83%) — S.F. 110 °C 40 min a

(93%) n-TSA — S.F. 110 °C 120 min a

S.F. 110 °C 180 min a — TS-1 (93%)

S.F. 80 °C 120 min b — CoFe₂O₄@Eggshell@SO₃H (95%)

B

Cp₂TiCl₂ + POAP (97%) — S.F. 25 °C 6 h a

Fe₃O₄@SiO₂@PrSO₃H (92%) — S.F. 25 °C 4 h a

Alginic acid aerogel (90%) — CH₃CN-H₂O 25 °C 19 h a

(93%) Hf(OTf)₄ — S.F. 25 °C 4 h a

MeOH 25 °C 2.1 h a — PS/TiCl₄ (93%)

EtOH 40 °C 3 h b — CoFe₂O₄@Eggshell@SO₃H (95%)

C

CoFe₂O₄@Eggshell@SO₃H (97%) — S.F. 80 °C 20 min b

(93%) Cu@imineZCMNPs — S.F. 80 °C 18 min a

EtOH Ref. 60 min a — (85 %) PDMAF-MNPs

Fe₃O₄@TiO₂@O₂PO₂(CH₂)NHSO₃H (90%) — S.F 90 °C 20 min a

(90%) GO — H₂O 80 °C 300 min a

S.F. 80 °C 20 min a — Nanomagnetic bearing morpholine tags (85%)

Fig. 10 A: [a] Comparison of the activity of some catalysts in 2,4,6-triarylpyridine reaction of benzaldehyde, ammonium acetate and acetophenone. (Tabrizian et al., 2015; Rekunge et al., 2018; Wang et al., 2019; Zolfigol et al., 2018; Gadekar and Lande, 2018) [b] (Benzyl alcohol, ammonium acetate, and acetophenone). B: [a] Comparison of activity of some catalysts in β-amino carbonyl reaction of benzaldehyde, aniline and acetophenone. (Rahmatpour et al., 2019; Zhu et al., 2015; Yeszhanov et al., 2018; Han et al., 2020; Pettignano et al., 2015) [b] (Benzyl alcohol, aniline, and acetophenone). C: [a] Comparison of activity of some catalysts in 2-amino-4,6-diphenylnicotinonitrile reaction of benzaldehyde, aniline and acetophenone. (Yahyazadeh et al., 2018; Zolfigol and Yarie, 2017; Khalili, 2016; Kalhor et al., 2019; Bodaghifard et al., 2017) [b] (Benzyl alcohol; malononitrile, ammonium acetate, and acetophenone).

@Eggshell@SO₃H nanocomposite was investigated in model reactions under optimized reaction conditions. After finish reaction, EtOAc was added to the reaction mixture, and the catalyst was isolated by an external magnet, washed with EtOH and EtOAc (2 × 5 mL), and dried under vacuum. The catalyst was successfully recycled five times and the turnover number (TON) in all these five periods is specified. The results showed that this CoFe₂O₄@Eggshell@SO₃H nanocomposite could be easily recovered and reused for several times without significant loss of activity or performance (Fig. 11).

The recyclability of CoFe₂O₄@Eggshell@SO₃H in the model 2,4,6-triarylpyridine reaction was studied. After each run, CoFe₂O₄@Eggshell@SO₃H was separated by a magnet, and washed with EtOH, and finally, dried overnight. Figure S1 shows the satisfactory reusability of the nanocomposite in this reaction (Figure S1 seen in SI file). CoFe₂O₄@Eggshell@SO₃-H was proved to be very robust. No significant deactivation was observed during the analogous five reaction cycles. The FESEM image, XRD and FT-IR spectrum of the reused catalyst after 5 cycles are shown in Figure S1a-c. The results were
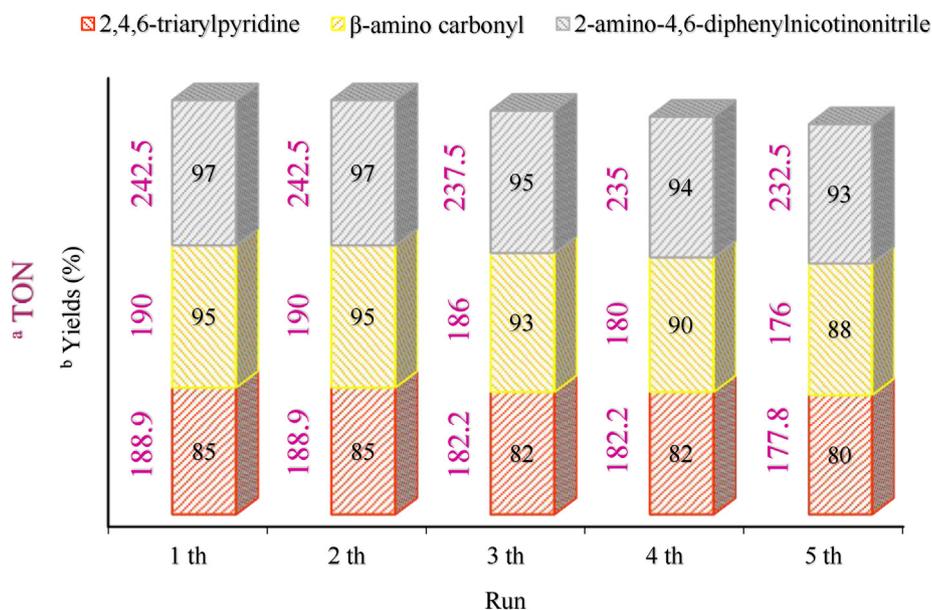
Fig. 11 Recovery of nanocomposite in 5 runs for all three model reactions; 2,4,6-triarylpyridine (red), β-amino carbonyl (yellow), and 2-amino-4,6-diphenylnicotinonitrile (blue) [a] Turnover number; [b] Isolated yield.

Table 6 $CoFe_2O_4$@Eggshell@SO_3H nanocomposite leaching test in model reactions.

Entry	Model reactions	Yields (%) Before of leaching test	Yields (%) After of leaching test
1 a	2,4,6-triarylpyridine	50	20
2b	β-amino carbonyl	95	45
3c	2-amino-4,6-diphenylnicotinonitrile	65	30

[a] Reaction conditions: Benzyl alcohol (1 mmol), Acetophenone (2 mmol), Ammonium acetate (1 mmol), EtOH., 80 °C, Catalyst (0.05 g), air as the oxidant.
[b] Reaction conditions: Benzyl alcohol (1 mmol), Acetophenone (1.2 mmol), Aniline (1 mmol), EtOH., 40 °C, Catalyst (0.08 g), air as the oxidant.
[c] Reaction conditions: Benzyl alcohol (1 mmol), Acetophenone (2 mmol), Ammonium acetate (1 mmol), malononitrile (1 mmol), CH_2Cl_2., 80 °C, Catalyst (0.06 g), air as the oxidant.

observed to be exactly the same as the pre-reaction spectrum, which indicates the high stability of the nanocomposite in the reaction path (Fig. S1: see in SI file). In order to investigate the heterogeneity of $CoFe_2O_4$@Eggshell@SO_3H nanocomposite during the reaction, leaching test for model reactions such as 6,4,4-triphenylpyridine in the presence of EtOH (benzyl alcohol/ acetophenone/ammonium acetate), β-aminocarbonyl in the presence of EtOH (benzyl alcohol/acetophenone/aniline) and 2-amino-4,6-diphenylnicotinonitrile in the presence of CH_2Cl_2 (benzyl alcohol/acetophenone/ ammonium acetate/-malononitrile) were performed. The nanocomposite was magnetically removed in situ after half of the reaction time (50 % conversion) from model reactions and the reactants were allowed to undergo further reaction (for 2,4,6-triarylpyridine after 50 % conversion: 20 % yields; for β-amino carbonyl after 50 % conversion: 45 % yields; for 2-amino-4,6-diphenylnicoti nonitrile after 50 % conversion: 30 % yields). These results indicated that after the removal of the heterogeneous catalyst, no progress was observed in any of the reactions, indicating the absence of the nanocomposite in the reaction medium and confirming that the synthesized acid nanocomposite acts heterogeneously in the reaction (Table 6).

4. Conclusion

In total, the current study found a path to the alteration of eggshell waste to a worthy solid catalyst. The functionalization of chlorosulfuric acid on core-shell $CoFe_2O_3$@eggshell gives a heterogeneous, green and recyclable solid acid catalyst for the synthesis of Hantzsh pyridine, and Mannich compounds of various aromatic alcohol are reported for the first time. Furthermore, the prevailing synthesis technique is a type of green, powerful, easy, economical, and environmental strategy for the preparation of other composites with eggshells, and other biomaterials as supports. The highlights of this work were simple work-up procedures, ease of preparation and facile purification, improved product yields, mild reaction conditions, shorter reaction times and recyclability of the catalyst at least 5th times are the main advantages of $CoFe_2O_4$@Eggshell@SO_3H nano-composite. I hope this work motivates researchers to prepare catalysts from the available waste international. So, research and experimentation into waste-to-wealth conversion are strongly encouraged.

Declaration of Competing Interest

The authors declare that they have no known competing financial interests or personal relationships that could have appeared to influence the work reported in this paper.

Acknowledgments

Appendix A. Supplementary material

Support information is available for free. All chemicals and device specifications, CHN and 1H NMR spectral information is located in the supporting information. Supplementary data to this article can be found online at https://doi.org/10.1016/j.arabjc.2023.104564.

References

Afzalimir, S.H., Barbosa, V.S., Ruggieri, C., 2020. Evaluation of CTOD resistance curves in clamped SE(T) specimens with weld centerline cracks. Eng. Fract. Mech. 240, 107326 https://doi.org/10.1016/j.engfracmech.2020.107326.

Alavinia, S., Ghorbani-Vaghei, R., 2022. Magnetic Fe₃O₄ nanoparticles in melamine-based ternary deep eutectic solvent as a novel eco-compatible system for green synthesis of pyrido[2,3-d]pyrimidine derivatives. J. Mol. Struct. 1270 133860. https://doi.org/10.1016/j.molstruc.2022.133860.

Ardeshir Khazaei, A.-R.-M.-Z., Gohari-Ghalil, F., Tavasoli, M., Rezaei-Gohar, M., 2020. Fe₃O₄ bonded Pyridinium-3-carboxylic acid-N-sulfonic Acid Chloride as an efficient catalyst for the synthesis of 3,4-dihydropyrimidin-2(1H)-ones. Chem. Methodol. 4, 543–553. https://doi.org/10.22034/chemm.2020.106433.

Bagherzade, G., Bakhshi, O., Ghamari Kargar, P., 2021. Biosynthesis of organic nanocomposite using Pistacia Vera L. hull: An efficient antimicrobial agent. Medbiotech J 5, 41–48 https://doi.org/10.22034/MBT.2021.135222.

Bagherzade, G., Khashei Siuki, H., gherzade and Khashei Siuki. Use of pectin as a suitable substrate for catalyst synthesis Fe₃O₄@-Pectin@Ni (II) and its application in oxidation reaction. Medbiotech J. 05, 1–8. https://doi.org/10.22034/mbt.2021.135147.

Bakavoli, M., Bagherzadeh, G., Rahimizadeh, M., 2005. Synthesis of optically active imidazo[1,2-a]pyrimidin-3(2H)-ones. Mendeleev Commun. 15, 145–146. https://doi.org/10.1070/MC2005v015n04ABEH001994.

Bakherad, M., Keivanloo, A., Amin, A.H., Ghamari Kargar, P., 2018. Silica-anchored Cu(I) aminothiophenol complex: An efficient heterogeneous catalyst for synthesis of 1,4-disubstituted 1,2,3-triazoles in water. Iran. J. Catal. 8 (3), 179–187.

Bakhshi, O., Bagherzade, G., Ghamari kargar, P., 2021. Biosynthesis of organic nanocomposite using Pistacia vera L. Hull: an efficient antimicrobial agent. Bioinorg. Chem. Appl. 2021, 1–18. https://doi.org/10.1155/2021/4105853.

Bita Baghernejad, M.R.H., 2021. Nano-cerium oxide/aluminum oxide: an efficient and useful catalyst for the synthesis of Tetrahydro[a]xanthenes-11-one derivatives. Chem. Methodol. 5, 90–95. https://doi.org/10.22034/chemm.2021.119641.

Bodaghifard, M.A., Asadbegi, S., Bahrami, Z., 2017. (Triazinediyl) bis sulfamic acid-functionalized silica-coated magnetite nanoparticles: preparation, characterization and application as an efficient catalyst for synthesis of mono-, bis-, tris- and spiro-perimidines. J. Iran. Chem. Soc. 14, 365–376. https://doi.org/10.1007/s13738-016-0985-9.

Caetano, C.S., Guerreiro, L., Fonseca, I.M., Ramos, A.M., Vital, J., Castanheiro, J.E., 2009. Esterification of fatty acids to biodiesel over polymers with sulfonic acid groups. Appl. Catal. A Gen. 359, 41–46. https://doi.org/10.1016/j.apcata.2009.02.028.

Erşatır, M., Yıldırım, M., 2021. Green synthesis of 2-amino-3-cyanopyridines via a cooperative vinylogous anomeric-based oxidation and their antiproliferative effects on liver, breast, and prostate cancer studies. Synth. Commun., 1–14 https://doi.org/10.1080/00397911.2021.1878537.

Fakhimi, R., Shahabsafa, M., Lei, W., He, S., Martins, J.R.R.A., Terlaky, T., Zuluaga, L.F., 2022. Discrete multi-load truss sizing optimization: model analysis and computational experiments. Optim. Eng. 23, 1559–1585 https://doi.org/10.1007/s11081-021-09672-6.

Fatemeh Kamali, F.S., 2021. Effective and convenient synthesis of 2-amino-4H-chromenes promoted by melamine as a recyclable organocatalyst. Eurasian Chem. Commun. 3, 278–290. https://doi.org/10.22034/ecc.2021.272326.1136.

Filho, J.F.A., Lemos, B.C., de Souza, A.S., Pinheiro, S., Greco, S.J., 2017. Multicomponent Mannich reactions: general aspects, methodologies and applications. Tetrahedron 73, 6977–7004. https://doi.org/10.1016/j.tet.2017.10.063.

Foroughi Kaldareh, M., Mokhtary, M., Nikpassand, M., 2020. Nicotinic acid-supported cobalt ferrite-catalyzed one-pot synthesis of substituted chromeno[3,4-b]quinolines. Appl. Organomet. Chem. 34. https://doi.org/10.1002/aoc.5469.

Gadekar, S.P., Lande, M.K., 2018. Solid acid catalyst TS-1 zeolite-assisted solvent-free one-pot synthesis of poly-substituted 2,4,6-triaryl-pyridines. Res. Chem. Intermed. 44, 3267–3278. https://doi.org/10.1007/s11164-018-3305-4.

Ghamari kargar, P., Bagherzade, G., 2021a. The anchoring of a Cu (ii)–salophen complex on magnetic mesoporous cellulose nanofibers: green synthesis and an investigation of its catalytic role in tetrazole reactions through a facile one-pot route. RSC Adv 11, 19203–19220 https://doi.org/10.1039/D1RA01913A.

Ghamari Kargar, P., Bagherzade, G., 2021b. Robust, highly active, and stable supported Co(ii) nanoparticles on magnetic cellulose nanofiber-functionalized for the multi-component reactions of piperidines and alcohol oxidation. RSC Adv. 11, 23192–23206. https://doi.org/10.1039/D1RA00208B.

Ghamari Kargar, P., Bagherzade, G., 2021c. A green synthesis strategy of binuclear catalyst for the C-C cross-coupling reactions in the aqueous medium: Hiyama and Suzuki-Miyaura reactions as case studies. Front. Chem. 9. https://doi.org/10.3389/fchem.2021.747016.

Ghamari Kargar, P., Aryanejad, S., Bagherzade, G., 2020a. Simple synthesis of the novel Cu-MOF catalysts for the selective alcohol oxidation and the oxidative cross-coupling of amines and alcohols. Appl. Organomet. Chem. 34. https://doi.org/10.1002/aoc.5965.

Ghamari Kargar, P., Bagherzade, G., Eshghi, H., 2020b. Novel biocompatible core/shell Fe₃O₄@NFC@Co(ii) as a new catalyst in a multicomponent reaction: an efficient and sustainable methodology and novel reusable material for one-pot synthesis of 4H-pyran and pyranopyrazole in aqueous media. RSC Adv. 10, 37086–37097. https://doi.org/10.1039/D0RA04698A.

Ghamari kargar, P., Bagherzade, G., Eshghi, H., 2020c. Design and synthesis of magnetic Fe₃O₄@NFC-ImSalophCu nanocatalyst based on cellulose nanofibers as a new and highly efficient, reusable, stable and green catalyst for the synthesis of 1,2,3-triazoles. RSC Adv 10, 32927–32937 https://doi.org/10.1039/D0RA06251K.

Ghamari kargar, P., Bagherzade, G., Beyzaei, H., 2022a. A porous metal-organic framework (Ni-MOF): An efficient and recyclable catalyst for cascade oxidative amidation of alcohols by amines under ultrasound-irradiations. Mol. Catal. 526, 112372 https://doi.org/10.1016/j.mcat.2022.112372.

Ghamari kargar, P., Bagherzade, G., Beyzaei, H., Arghavani, S., 2022b. BioMOF-Mn: An Antimicrobial Agent and an Efficient Nanocatalyst for Domino One-Pot Preparation of Xanthene Derivatives. Inorg. Chem. 61 (28), 10678–10693 https://doi.org/10.1021/acs.inorgchem.2c00819.

Ghamari Kargar, P., Nayebi, M., Parhizi, Z., Varma, R.S., 2022c. Nickel nanoparticles adorned on magnetized cellulose nanofibers: ultrasound-facilitated cross coupling reactions. Cellulose 29 (17), 9183–9198 https://doi.org/10.1007/s10570-022-04823-z.

Ghamari Kargar, P., Len, C., Luque, R., 2022d. Cu/cellulose-modified magnetite nanocomposites as a highly active and selective catalyst for ultrasound-promoted aqueous O-arylation Ullmann and sp-sp^2 Sonogashira cross-coupling reactions. Sustain. Chem. Pharm. 27,. https://doi.org/10.1016/j.scp.2022.100672 100672.

Ghamari kargar, P., Bagherzade, G., Eshghi, H., 2021a. Introduction of a trinuclear manganese(iii) catalyst on the surface of magnetic cellulose as an eco-benign, efficient and reusable novel heterogeneous catalyst for the multi-component synthesis of new derivatives of xanthene. RSC Adv 11, 4339–4355 https://doi.org/10.1039/D0RA09420J.

Ghamari Kargar, P., Ravanjamjah, A., Bagherzade, G., 2021b. A novel water-dispersible and magnetically recyclable nickel nanoparticles for the one-pot reduction-Schiff base condensation of nitroarenes in pure water. J. Chinese Chem. Soc. 68, 1916–1933 https://doi.org/10.1002/jccs.202100172.

Ghamari Kargar, P., Noorian, M., Chamani, E., Bagherzade, G., Kiani, Z., 2021c. Synthesis, characterization and cytotoxicity evaluation of a novel magnetic nanocomposite with iron oxide deposited on cellulose nanofibers with nickel (Fe3O4@NF-C@ONSM-Ni). RSC Adv. 11, 17413–17430. https://doi.org/10.1039/D1RA01256H.

Ghamari kargar, P., Ghasemi, M., Bagherzade, G., 2021d. Magnetic nanoparticles embedded in pectin-based as an environmentally friendly recyclable nanocatalyst. Medbiotech J 5, 9–14 https://doi.org/10.22034/MBT.2021.135148.

Ghamari Kargar, P., Bagherzade, G., Ghasemi, M., 2021. Copper (II), supported on a post-modified magnetic Pectin Fe$_3$O$_4$@-Pectin~Imidazole~SO$_3$H-Cu(II): an efficient biopolymer-based catalyst for selective oxidation of alcohols with aqueous TBHP. Sci. Iran. https://doi.org/10.24200/sci.2021.58355.5689.

Ghani, M., Khodkavandi, S., Jafari, Z., Ghamari kargar, P., Maleki, B., Fathnia Tabari, H., 2023. Synthesis of cellulose nanofibers-based ImSalophen@Fe$_3$O$_4$ as a green sorbent for magnetic solid-phase extraction of chlorophenols followed by quantification via high-performance liquid chromatography-ultraviolet detection. Microchem. J. 187, 108368 https://doi.org/10.1016/j.microc.2022.108368.

Ghazavi, M., Abdollahi, S.F., Kutay, M.E., 2022. Implementation of NCHRP 9-44A Fatigue Endurance Limit Prediction Model in Mechanistic-Empirical Asphalt Pavement Analysis Web Application. Transp. Res. Rec. J. Transp. Res. Board 2676, 696–706 https://doi.org/10.1177/03611981221076114.

Gholami, A., Mokhtary, M., Nikpassand, M., 2020. Glycolic acid-supported cobalt ferrite-catalyzed one-pot synthesis of pyrimido [4,5-b]quinoline and indenopyrido[2,3-d]pyrimidine derivatives. Appl. Organomet. Chem. 34. https://doi.org/10.1002/aoc.6007.

S. V. Goswami, P.B. Thorat, A. V. Chakrawar, S.R. Bhusare, A mild and efficient one-pot synthesis of β -amino carbonyl compounds via Mannich reaction under ambient temperature condition, Mol. Divers. 17 (2013) 33–40. https://doi.org/10.1007/s11030-012-9414-x.

Gu, Y., Karam, A., Jérôme, F., Barrault, J., 2007. Selectivity enhancement of silica-supported sulfonic acid catalysts in water by coating of ionic liquid. Org. Lett. 9, 3145–3148. https://doi.org/10.1021/ol071356j.

Hajizadeh, Z., Valadi, K., Taheri-Ledari, R., Maleki, A., 2020. Convenient Cr(VI) removal from aqueous samples: executed by a promising clay-based catalytic system, magnetized by Fe$_3$O$_4$ nanoparticles and functionalized with humic acid. ChemistrySelect 5, 2441–2448. https://doi.org/10.1002/slct.201904672.

Han, S.-B., Wei, J.-Y., Peng, X.-C., Liu, R., Gong, S.-S., Sun, Q., 2020. Hf(OTf)$_4$ as a highly potent catalyst for the synthesis of mannich bases under solvent-free conditions. Molecules 25, 388. https://doi.org/10.3390/molecules25020388.

Heravi, M.M., Yahya Shirazi Beheshtiha, S., Dehghani, M., Hosseintash, N., 2015. Using magnetic nanoparticles Fe3O4 as a reusable catalyst for the synthesis of pyran and pyridine derivatives via one-pot multicomponent reaction. J. Iran. Chem. Soc. 12, 2075–2081 https://doi.org/10.1007/s13738-015-0684-y.

Hayati, E., Abdi, E., Mohseni Saravi, M., Nieber, J.L., Majnounian, B., Chirico, G.B., 2018. How deep can forest vegetation cover extend their hydrological reinforcing contribution? Hydrol. Process. 32, 2570–2583 https://doi.org/10.1002/hyp.13174.

Hosseini, S., Khamesee, M.B., 2021. Modeling And Simulation And Imaging Of Blood Flow In The Human Body. NVEO-NATURAL VOLATILES Essent. OILS 8, 13235–13244.

Hosseinzadeh, Z., Ramazani, A., Ahankar, H., Ślepokura, K., Lis, T., 2019. Sulfonic acid-functionalized silica-coated magnetic nanoparticles as a reusable catalyst for the preparation of pyrrolidinone derivatives under eco-friendly conditions. Silicon 11, 2933–2943. https://doi.org/10.1007/s12633-019-0087-2.

Hosseinzadeh-Khanmiri, R., Kamel, Y., Keshvari, Z., Mobaraki, A., Shahverdizadeh, G.H., Vessally, E., Babazadeh, M., 2018. Synthesis and characterization of a Ni nanoparticle stabilized on Ionic liquid-functionalized magnetic Silica nanoparticles for tandem oxidative reaction of primary alcohols. Appl. Organomet. Chem. 32, e4452.

Jabbar, R., Sabeeh, S.H., Hameed, A.M., 2020. Structural, dielectric and magnetic properties of Mn + 2 doped cobalt ferrite nanoparticles. J. Magn. Magn. Mater. 494,. https://doi.org/10.1016/j.jmmm.2019.165726 165726.

Ji, S., Ran, R., Chiniforooshan Esfahani, I., Wan, K., Sun, H., 2021. A New Microfluidic Device Integrated With Quartz Crystal Microbalance to Measure Colloidal Particle Adhesion. In: Biomedical and Biotechnology, 5. American Society of Mechanical Engineers https://doi.org/10.1115/IMECE2021-73099.

Kalantari, F., Rezayati, S., Ramazani, A., Aghahosseini, H., Ślepokura, K., Lis, T., 2022. Proline-Cu complex based 1,3,5-Triazine coated on Fe$_3$O$_4$ magnetic nanoparticles: a nanocatalyst for the knoevenagel condensation of aldehyde with malononitrile. ACS Appl. Nano Mater. 5, 1783–1797. https://doi.org/10.1021/acsanm.1c03169.

Kalhor, S., Yarie, M., Rezaeivala, M., Zolfigol, M.A., 2019. Novel magnetic nanoparticles with morpholine tags as multirole catalyst for synthesis of hexahydroquinolines and 2-amino-4,6-diphenylnicotinonitriles through vinylogous anomeric-based oxidation. Res. Chem. Intermed. 45, 3453–3480. https://doi.org/10.1007/s11164-019-03802-7.

Kang, N., Xu, D., Han, Y., Lv, X., Chen, Z., Zhou, T., Ren, L., Zhou, X., 2019. Magnetic targeting core/shell Fe$_3$O$_4$/Au nanoparticles for magnetic resonance/photoacoustic dual-modal imaging. Mater. Sci. Eng. C. 98, 545–549. https://doi.org/10.1016/j.msec.2019.01.013.

Karaagac, O., Yildiz, B.B., Köçkar, H., 2019. The influence of synthesis parameters on one-step synthesized superparamagnetic cobalt ferrite nanoparticles with high saturation magnetization. J. Magn. Magn. Mater. 473, 262–267. https://doi.org/10.1016/j.jmmm.2018.10.063.

Khaksar, S., Yaghoobi, M., 2012. A concise and versatile synthesis of 2-amino-3-cyanopyridine derivatives in 2,2,2-trifluoroethanol. J. Fluor. Chem. 142, 41–44. https://doi.org/10.1016/j.jfluchem.2012.06.009.

Khalili, D., 2016. Graphene oxide: a reusable and metal-free carbocatalyst for the one-pot synthesis of 2-amino-3-cyanopyridines in water. Tetrahedron Lett. 57, 1721–1723. https://doi.org/10.1016/j.tetlet.2016.03.020.

Khashei Siuki, H., Bagherzade, G., Ghamari Kargar, P., 2020. A green method for synthesizing nickel nanoparticles supported by magnetized pectin: applied as a catalyst for aldehyde synthesis as a precursor in Xanthan synthesis. ChemistrySelect 5, 13537–13544. https://doi.org/10.1002/slct.202002946.

Khashei Siuki, H., Ghamari Kargar, P., Bagherzade, G., 2022. New Acetamidine Cu(II) Schiff base complex supported on magnetic nanoparticles pectin for the synthesis of triazoles using click chemistry. Sci. Rep. 12, 3771. https://doi.org/10.1038/s41598-022-07674-7.

Khazaei, A., Sarmasti, N., Seyf, J.Y., 2018. Waste to wealth: conversion of nano-magnetic eggshell (Fe_3O_4@Eggshell) to Fe_3O_4@$Ca(HSO_4)_2$: cheap, green and environment-friendly solid acid catalyst. Appl. Organomet. Chem. 32, e4308.

Kiani, M., Bagherzadeh, M., Meghdadi, S., Fadaei-Tirani, F., Babaie, M., Schenk-Joß, K., 2020. Promising new catalytic properties of a Co (II)-carboxamide complex and its derived Co_3O_4 nanoparticles for the Mizoroki-Heck and the Epoxidation reactions. Appl. Organomet. Chem. 34. https://doi.org/10.1002/aoc.5911.

Kim, B.Y., Ahn, J.B., Lee, H.W., Kang, S.K., Lee, J.H., Shin, J.S., Ahn, S.K., Il Hong, C., Yoon, S.S., 2004. Synthesis and biological activity of novel substituted pyridines and purines containing 2,4-thiazolidinedione. Eur. J. Med. Chem. 39, 433–447. https://doi.org/10.1016/j.ejmech.2004.03.001.

Kundu, K., Nayak, S.K., 2012. (±)-Camphor-10-sulfonic acid catalyzed direct one-pot three-component Mannich type reaction of alkyl (hetero)aryl ketones under solvent-free conditions: application to the synthesis of aminochromans. RSC Adv. 2, 480–486. https://doi.org/10.1039/C1RA00652E.

Londoño-Calderón, C.L., Londoño-Calderón, A., Menchaca-Nal, S., Salazar-Henao, N.A., Rosales-Rivera, A., Pampillo, L.G., Martínez-García, R., 2020. Magnetic properties of cobalt ferrite octahedrons obtained from calcination of granular nanotubes growing on bacterial nanocellulose. J. Magn. Magn. Mater. 495. https://doi.org/10.1016/j.jmmm.2019.165899 165899.

Lu, G., Cai, C., 2010. Mannich reactions catalyzed by perchloric acid in Triton X10 aqueous micelles. Catal. Commun. 11, 745–748. https://doi.org/10.1016/j.catcom.2010.02.007.

Lu, Y., Lu, X., Mayers, B.T., Herricks, T., Xia, Y., 2008. Synthesis and characterization of magnetic Co nanoparticles: a comparison study of three different capping surfactants. J. Solid State Chem. 181, 1530–1538. https://doi.org/10.1016/j.jssc.2008.02.016.

Mahhouti, Z., El Moussaoui, H., Mahfoud, T., Hamedoun, M., El Marssi, M., Lahmar, A., El Kenz, A., Benyoussef, A., 2019. Chemical synthesis and magnetic properties of monodisperse cobalt ferrite nanoparticles. J. Mater. Sci. Mater. Electron. 30, 14913–14922. https://doi.org/10.1007/s10854-019-01863-3.

Mahmoudiani Gilan, M., Khazaei, A., Sarmasti, N., 2021. Utilization of eggshell waste as green catalyst for application in the synthesis of 1,2,4,5-tetra-substituted imidazole derivatives. Res. Chem. Intermed. 47, 2173–2188. https://doi.org/10.1007/s11164-018-03724-w.

Milam-Guerrero, J., Neer, A.J., Melot, B.C., 2019. Crystal chemistry and competing magnetic exchange interactions in oxide garnets and spinels. J. Solid State Chem. 274, 1–9. https://doi.org/10.1016/j.jssc.2019.02.007.

Mohammadi, R., Eidi, E., Ghavami, M., Kassaee, M.Z., 2014. Chitosan synergistically enhanced by successive Fe3O4 and silver nanoparticles as a novel green catalyst in one-pot, three-component synthesis of tetrahydrobenzo[α]xanthene-11-ones. J. Mol. Catal. A Chem. 393, 309–316. https://doi.org/10.1016/j.molcata.2014.06.005.

Mohammadi Ziarani, G., Kheilkordi, Z., Mohajer, F., Badiei, A., Luque, R., 2021. Magnetically recoverable catalysts for the preparation of pyridine derivatives: an overview. RSC Adv. 11, 17456–17477. https://doi.org/10.1039/D1RA02418C.

Morales, G., Paniagua, M., Melero, J.A., Vicente, G., Ochoa, C., 2011. Sulfonic acid-functionalized catalysts for the valorization of glycerol via transesterification with methyl acetate. Ind. Eng. Chem. Res. 50, 5898–5906. https://doi.org/10.1021/ie102357c.

Nabizadeh, M., Jamali, S., 2021. Life and death of colloidal bonds control the rate-dependent rheology of gels. Nat. Commun. 12, 4274 https://doi.org/10.1038/s41467-021-24416-x.

Naeimi, H., Nazifi, Z.S., 2014. Sulfonated diatomite as heterogeneous acidic nanoporous catalyst for synthesis of 14-aryl-14-H-dibenzo[a,j]xanthenes under green conditions. Appl. Catal. A Gen. 477, 132–140. https://doi.org/10.1016/j.apcata.2014.03.012.

Nagarapu, L., Aneesa, R., Peddiraju, S., 2007. Apuri, $HClO_4$–SiO_2 as a novel and recyclable catalyst for the synthesis of 2,4,6-triarylpyridines under solvent-free conditions. Catal. Commun. 8, 1973–1976. https://doi.org/10.1016/j.catcom.2007.08.003.

Nasrollahzadeh, M., Sajadi, S.M., Hatamifard, A., 2016. Waste chicken eggshell as a natural valuable resource and environmentally benign support for biosynthesis of catalytically active Cu/eggshell, Fe_3O_4/eggshell and Cu/Fe_3O_4/eggshell nanocomposites. Appl. Catal. B Environ. 191, 209–227. https://doi.org/10.1016/j.apcatb.2016.02.042.

Pettignano, A., Bernardi, L., Fochi, M., Geraci, L., Robitzer, M., Tanchoux, N., Quignard, F., 2015. Alginic acid aerogel: a heterogeneous Brønsted acid promoter for the direct Mannich reaction. New J. Chem. 39, 4222–4226. https://doi.org/10.1039/C5NJ00349K.

Pi, Y., Gao, H., Cao, Y., Cao, R., Wang, Y., Sun, J., 2020. Cobalt ferrite supported on carbon nitride matrix prepared using waste battery materials as a peroxymonosulfate activator for the degradation of levofloxacin hydrochloride. Chem. Eng. J. 379,. https://doi.org/10.1016/j.cej.2019.122377 122377.

Radmansouri, M., Bahmani, E., Sarikhani, E., Rahmani, K., Sharifianjazi, F., Irani, M., 2018. Doxorubicin hydrochloride - loaded electrospun chitosan/cobalt ferrite/titanium oxide nanofibers for hyperthermic tumor cell treatment and controlled drug release. Int. J. Biol. Macromol. 116, 378–384. https://doi.org/10.1016/j.ijbiomac.2018.04.161.

Rahmatpour, A., Eeimen, R., Goodarzi, N., 2019. Titanium tetrachloride incorporated crosslinked polystyrene copolymer as an efficient and recyclable polymeric Lewis acid catalyst for the synthesis of B -amino carbonyl compounds at room temperature. Synth. Commun., 1–16 https://doi.org/10.1080/00397911.2019.1650379.

Rekunge, D.S., Kale, I.A., Chaturbhuj, G.U., 2018. An efficient, green solvent-free protocol for the synthesis of 2,4,6-triarylpyridines using reusable heterogeneous activated Fuller's earth catalyst. J. Iran. Chem. Soc. 15, 2455–2462. https://doi.org/10.1007/s13738-018-1434-8.

Rekunge, D.S., Mali, A.S., Chaturbhuj, G.U., 2021. One-pot expeditious synthesis of 2-Amino-4,6-(disubstituted)nicotinonitriles using activated fuller's Earth as catalyst. Org. Prep. Proced. Int. 53, 112–119. https://doi.org/10.1080/00304948.2020.1858693.

A. reza M. Jalal Albadi, Heshmat allah Samimi, Alumina-Supported Cobalt Nanoparticles Efficiently Catalyzed the Synthesis of Chromene Derivatives under Solvent-Free Condition, Chem. Methodol. 4 (2020) 565–571. https://doi.org/https://doi.org/10.22034/chemm.2020.107071.

Rezayati, S., Ramazani, A., Sajjadifar, S., Aghahosseini, H., Rezaei, A., 2021. Design of a Schiff Base complex of copper coated on epoxy-modified core-shell MNPs as an environmentally friendly and novel catalyst for the one-pot synthesis of various chromene-annulated heterocycles. ACS Omega 6, 25608–25622. https://doi.org/10.1021/acsomega.1c03672.

Rezayati, S., Kalantari, F., Ramazani, A., Sajjadifar, S., Aghahosseini, H., Rezaei, A., 2022. Magnetic silica-coated picolylamine copper complex [Fe_3O_4@SiO_2 @GP/Picolylamine-Cu(II)]-catalyzed Biginelli Annulation reaction. Inorg. Chem. 61, 992–1010. https://doi.org/10.1021/acs.inorgchem.1c03042.

Rostamnia, S., Doustkhah, E., 2015. Increased SBA-15-SO₃H catalytic activity through hydrophilic/hydrophobic fluoroalkyl-chained alcohols (RFOH/SBA-15–Pr-SO₃H). Synlett 26, 1345–1347. https://doi.org/10.1055/s-0034-1380683.

Rouhani, A.R., Esmaeil-Khanian, A.H., Davar, F., Hasani, S., 2018. The effect of agarose content on the morphology, phase evolution, and magnetic properties of CoFe₂O₄nanoparticles prepared by sol-gel autocombustion method. Int. J. Appl. Ceram. Technol. 15, 758–765. https://doi.org/10.1111/ijac.12832.

Safari, J., Javadian, L., 2015. Ultrasound assisted the green synthesis of 2-amino-4H-chromene derivatives catalyzed by Fe₃O₄-function-alized nanoparticles with chitosan as a novel and reusable magnetic catalyst. Ultrason. Sonochem. 22, 341–348. https://doi.org/10.1016/j.ultsonch.2014.02.002.

Safari, J., Banitaba, S.H., Khalili, S.D., 2012. Ultrasound-promoted an efficient method for one-pot synthesis of 2-amino-4,6-diphenyl-nicotinonitriles in water: a rapid procedure without catalyst. Ultrason. Sonochem. 19, 1061–1069. https://doi.org/10.1016/j.ultsonch.2012.01.005.

Seitllari, A., Ghazavi, M., Kutay, M.E., 2020. Effects of Binder Modification on Rutting Performance of Asphalt Binders https://doi.org/10.1007/978-3-030-48679-2_57.

Sharifianjazi, F., Moradi, M., Parvin, N., Nemati, A., Jafari Rad, A., Sheysi, N., Abouchenari, A., Mohammadi, A., Karbasi, S., Ahmadi, Z., Esmaeilkhanian, A., Irani, M., Pakseresht, A., Sahmani, S., Shahedi Asl, M., 2020. Magnetic CoFe₂O₄ nanoparticles doped with metal ions: a review. Ceram. Int. 46, 18391–18412. https://doi.org/10.1016/j.ceramint.2020.04.202.

Sharma, U.K., Ranjan, P., Van der Eycken, E.V., You, S.-L., 2020. Sequential and direct multicomponent reaction (MCR)-based dearomatization strategies. Chem. Soc. Rev. 49, 8721–8748. https://doi.org/10.1039/D0CS00128G.

H. Stadelman, W. J., & Schmieder, Functional uses of eggs: An overview. Eggs and health promotion, (2002) 3–8.

Sobhaniaragh, B., Afzalimir, S.H., Ruggieri, C., 2021. Towards the prediction of hydrogen–induced crack growth in high–graded strength steels. Thin-Walled Struct 159, 107245 https://doi.org/10.1016/j.tws.2020.107245.

Tabrizian, E., Amoozadeh, A., Rahmani, S., Imanifar, E., Azhari, S., Malmir, M., 2015. One-pot, solvent-free and efficient synthesis of 2,4,6-triarylpyridines catalyzed by nano-titania-supported sulfonic acid as a novel heterogeneous nanocatalyst. Chinese Chem. Lett. 26, 1278–1282. https://doi.org/10.1016/j.cclet.2015.06.013.

Taheri, S., Veisi, H., Hekmati, M., 2017. Application of poly-dopamine sulfamic acid-functionalized magnetic Fe₃O₄ nanoparticles (Fe₃O₄@PDA-SO₃H) as a heterogeneous and recyclable nanocatalyst for the formylation of alcohols and amines under solvent-free conditions. New J. Chem. 41, 5075–5081. https://doi.org/10.1039/C7NJ00417F.

Taheri-Ledari, R., Zhang, W., Radmanesh, M., Mirmohammadi, S. S., Maleki, A., Cathcart, N., Kitaev, V., 2020. Multi-stimuli nanocomposite therapeutic: docetaxel targeted delivery and synergies in treatment of human breast cancer tumor. Small 16, 2002733. https://doi.org/10.1002/smll.202002733.

S. Talha, N. S., & Sulaiman, Overview of catalysts in biodiesel production., ARPN J. Eng. Appl. Sci. 11 (2016) 439–442.

V.N.K. and B.R. J. Venu Madhav, P. Someshwar, Dipyridine copper chloride-catalysed one-pot synthesis of β-amino carbonyl compounds via Mannich reaction, J. Chem. Res. (2008) 201–202.

Wang, P.-L., Ding, S.-Y., Zhang, Z.-C., Wang, Z.-P., Wang, W., 2019. Constructing robust covalent organic frameworks via multicomponent reactions. J. Am. Chem. Soc. 141, 18004–18008. https://doi.org/10.1021/jacs.9b10625.

Wang, H., Zhao, W., Du, J., Wei, F., Chen, Q., Wang, X., 2019. Cationic organotin cluster [t -Bu₂Sn(OH)(H₂O)]22+ 2OTf − -

catalyzed one-pot three-component syntheses of 5-substituted 1 H -tetrazoles and 2,4,6-triarylpyridines in water. Appl. Organomet. Chem. 33. https://doi.org/10.1002/aoc.5132.

Xie, W., Gao, C., Li, J., 2021. Sustainable biodiesel production from low-quantity oils utilizing H₆PV₃MoW₈O₄₀ supported on magnetic Fe₃O₄/ZIF-8 composites. Renew. Energ. 168, 927–937. https://doi.org/10.1016/j.renene.2020.12.129.

Xie, W., Wang, H., 2021. Grafting copolymerization of dual acidic ionic liquid on core-shell structured magnetic silica: a magnetically recyclable Brönsted acid catalyst for biodiesel production by one-pot transformation of low-quality oils. Fuel 283,. https://doi.org/10.1016/j.fuel.2020.118893 118893.

Yahyazadeh, A., Abbaspour-Gilandeh, E., Aghaei-Hashjin, M., 2018. Four-component synthesis of 2-Amino-3-Cyanopyridine derivatives catalyzed by Cu@imineZCMNPs as a novel, efficient and simple nanocatalyst under solvent-free conditions. Catal. Lett. 148, 1254–1262. https://doi.org/10.1007/s10562-018-2318-3.

Yeszhanov, A.B., Mashentseva, A.A., Korolkov, I.V., Gorin, Y.G., Kozlovskiy, A.L., Zdorovets, M.V., 2018. Copper nanotube composite membrane as a catalyst in Mannich reaction. Chem. Pap. 72, 3189–3194. https://doi.org/10.1007/s11696-018-0539-y.

Zafari, S., Ghorbani-Vaghei, R., Alavinia, S., 2021. Poly(sulfon-amide-thiourea) grafted γ-Fe₂O₃@talc as a green catalyst for the synthesis of substituted tetrahydropyridines. Mater. Chem. Phys. 270,. https://doi.org/10.1016/j.matchemphys.2021.124840 124840.

Zareyee, D., Moosavi, S.M., Alaminezhad, A., 2013. Chemoselective synthesis of geminal diacetates (acylals) using eco-friendly reusable propylsulfonic acid based nanosilica (SBA-15-Ph-PrSO₃H) under solvent-free conditions. J. Mol. Catal. A Chem. 378, 227–231. https://doi.org/10.1016/j.molcata.2013.07.001.

Zareyee, D., Serehneh, M., 2014. Recyclable CMK-5 supported sulfonic acid as an environmentally benign catalyst for solvent-free one-pot construction of coumarin through Pechmann condensation. J. Mol. Catal. A Chem. 391, 88–91. https://doi.org/10.1016/j.molcata.2014.04.013.

Zhang, W., Taheri-Ledari, R., Hajizadeh, Z., Zolfaghari, E., Ahghari, M.R., Maleki, A., Hamblin, M.R., Tian, Y., 2020. Enhanced activity of vancomycin by encapsulation in hybrid magnetic nanoparticles conjugated to a cell-penetrating peptide. Nanoscale 12, 3855–3870. https://doi.org/10.1039/C9NR09687F.

Zhang, Z., Zhu, Y., Zhou, C., Liu, Q., Lu, H., Ge, Y., Wang, M., 2014. Development of β-amino-carbonyl compounds as androgen receptor antagonists. Acta Pharmacol. Sin. 35, 664–673. https://doi.org/10.1038/aps.2013.201.

Zhu, X., Chen, C., Yu, B., Wu, Y., Zhang, G., Zhang, W., Gao, Z., 2015. Titanocene dichloride and poly(o-aminophenol) as a new heterogeneous cooperative catalysis system for three-component Mannich reaction, Catal. Sci. Technol. 5, 4346–4349. https://doi.org/10.1039/C5CY00793C.

Zolfigol, M.A., Navazeni, M., Yarie, M., Ayazi-Nasrabadi, R., 2016. Application of biological-based nano and nano magnetic catalysts in the preparation of arylbispyranylmethanes. RSC Adv. 6, 92862–92868. https://doi.org/10.1039/C6RA18719F.

Zolfigol, M.A., Karimi, F., Yarie, M., Torabi, M., 2018. Catalytic application of sulfonic acid-functionalized titana-coated magnetic nanoparticles for the preparation of 1,8-dioxodecahydroacridines and 2,4,6-triarylpyridines via anomeric-based oxidation. Appl. Organomet. Chem. 32. https://doi.org/10.1002/aoc.4063.

Zolfigol, M.A., Yarie, M., 2017. Fe₃O₄@TiO₂@O₂PO₂ (CH₂) NHSO₃ H as a novel nanomagnetic catalyst: Application to the preparation of 2-amino-4,6-diphenylnicotinonitriles via anomeric-based oxidation. Appl. Organomet. Chem. 31, e3598.